Physics Letters B 725 (2013) 243–270

Contents lists available at SciVerse ScienceDirect

Physics Letters B

www.elsevier.com/locate/physletb

Search for gluino mediated bottom- and top-squark production in multijet final states in pp collisions at 8 TeV

CMS Collaboration *

CERN, Switzerland

ARTICLE INFO

Article history:
Received 10 May 2013
Received in revised form 26 June 2013
Accepted 27 June 2013
Available online 4 July 2013
Editor: M. Doser

Keywords:
CMS
Physics
SUSY
Hadronic
Btag

ABSTRACT

A search for supersymmetry is presented based on events with large missing transverse energy, no isolated electron or muon, and at least three jets with one or more identified as a bottom-quark jet. A simultaneous examination is performed of the numbers of events in exclusive bins of the scalar sum of jet transverse momentum values, missing transverse energy, and bottom-quark jet multiplicity. The sample, corresponding to an integrated luminosity of 19.4 fb^{-1}, consists of proton–proton collision data recorded at a center-of-mass energy of 8 TeV with the CMS detector at the LHC in 2012. The observed numbers of events are found to be consistent with the standard model expectation, which is evaluated with control samples in data. The results are interpreted in the context of two simplified supersymmetric scenarios in which gluino pair production is followed by the decay of each gluino to an undetected lightest supersymmetric particle and either a bottom or top quark–antiquark pair, characteristic of gluino mediated bottom- or top-squark production. Using the production cross section calculated to next-to-leading-order plus next-to-leading-logarithm accuracy, and in the limit of a massless lightest supersymmetric particle, we exclude gluinos with masses below 1170 GeV and 1020 GeV for the two scenarios, respectively.

1. Introduction

The standard model (SM) of particle physics has proved to be remarkably successful in describing phenomena up to the highest energy scales that have been probed. Nonetheless, the SM is widely viewed to be incomplete. Many extensions have been proposed to provide a more fundamental theory. Supersymmetry (SUSY) [1–8], one such extension, postulates that each SM particle is paired with a SUSY partner from which it differs in spin by one-half unit, with otherwise identical quantum numbers. For example, squarks and gluinos are the SUSY partners of quarks and gluons, respectively. One of the principal motivations for SUSY is to stabilize the calculation of the Higgs boson mass. For this stabilization to be "natural" [9–11], top squarks, bottom squarks, and to a lesser extent gluinos, must be relatively light. If top and bottom squarks are light, their production is enhanced, either through direct pair production or through production mediated by gluinos, where the latter process is favored if the gluino is relatively light so that its pair production cross section is large. Since the decay products of both bottom and top squarks include bottom quarks, natural SUSY models are characterized by an abundance of bottom-quark jets (b jets).

In R-parity-conserving [12] SUSY models, supersymmetric particles are created in pairs. Each member of the pair initiates a decay chain that terminates with the lightest SUSY particle (LSP) and SM particles, typically including quarks and gluons, which then hadronize to form jets. If the LSP only interacts weakly, as in the case of a dark-matter candidate, it escapes detection, potentially yielding significant missing transverse energy ($E_{\mathrm{T}}^{\mathrm{miss}}$). Thus large values of $E_{\mathrm{T}}^{\mathrm{miss}}$ provide another possible SUSY signature.

In this Letter, we present a search for SUSY in events with at least three jets, one or more of which are identified as b jets (b tagged), and large $E_{\mathrm{T}}^{\mathrm{miss}}$. The search is based on a sample of proton–proton (pp) collision data collected at $\sqrt{s} = 8$ TeV with the Compact Muon Solenoid (CMS) detector at the CERN Large Hadron Collider (LHC) in 2012, corresponding to an integrated luminosity of 19.4 fb^{-1}. Previous LHC new-physics searches in final states with b jets and $E_{\mathrm{T}}^{\mathrm{miss}}$ are presented in Refs. [13–25]. The current analysis is an extension of the study presented in Ref. [23], which was based on 4.98 fb^{-1} of data collected at $\sqrt{s} = 7$ TeV. We retain the same basic analysis procedures, characterized by a strong reliance on control samples in data, to evaluate the SM backgrounds. The principal backgrounds arise from the production of events with a top quark–antiquark ($t\bar{t}$) pair, a single-top quark,

* *E-mail address:* cms-publication-committee-chair@cern.ch.

0370-2693/
http://dx.doi.org/10.1016/j.physletb.2013.06.058

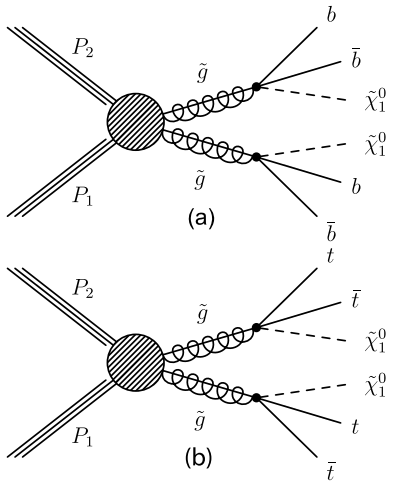

Fig. 1. Event diagrams for the (a) T1bbbb and (b) T1tttt simplified SUSY scenarios.

a W boson in association with jets (W + jets), a Z boson in association with jets (Z + jets), and multiple jets produced through the strong interaction, in which a b-tagged jet is present. We refer to events in the latter category as quantum chromodynamics (QCD) multijet events. For W + jets events and events with top quarks, significant $E_{\mathrm{T}}^{\mathrm{miss}}$ can arise if a W boson decays into a neutrino and a charged lepton. The neutrino provides a source of genuine $E_{\mathrm{T}}^{\mathrm{miss}}$. For events with a Z boson, significant $E_{\mathrm{T}}^{\mathrm{miss}}$ can arise if the Z boson decays to two neutrinos. For QCD multijet events, significant $E_{\mathrm{T}}^{\mathrm{miss}}$ can arise when a charm or bottom quark undergoes semileptonic decay, but the main source of $E_{\mathrm{T}}^{\mathrm{miss}}$ is a mismeasurement of jet transverse momentum p_{T}. The QCD multijet category excludes events that are contained in the other categories.

As new-physics scenarios, we consider the simplified SUSY spectra [26–29] in which gluino pair production is followed by the decay of each gluino $\tilde{\mathrm{g}}$ into a bottom quark and an off-shell bottom squark or into a top quark and an off-shell top squark. The off-shell bottom (top) squark decays into a bottom (top) quark and the LSP, where the LSP is assumed to escape detection, leading to significant $E_{\mathrm{T}}^{\mathrm{miss}}$. A possible LSP candidate is the lightest neutralino $\tilde{\chi}_1^0$; we therefore use the symbol $\tilde{\chi}_1^0$ to denote the LSP. We assume all SUSY particles other than the gluino and the LSP to be too heavy to be produced at current LHC energies, and the gluino to be short-lived. The production cross section is computed [30–34] at the next-to-leading-order (NLO) plus next-to-leading-logarithm (NLL) level. We denote the $\tilde{\mathrm{g}}\tilde{\mathrm{g}} \to 2 \times \mathrm{b\bar{b}}\tilde{\chi}_1^0$ process as the T1bbbb scenario and the $\tilde{\mathrm{g}}\tilde{\mathrm{g}} \to 2 \times \mathrm{t\bar{t}}\tilde{\chi}_1^0$ process as the T1tttt scenario [35]. Event diagrams are shown in Fig. 1. If the bottom (top) squark is much lighter than any other squark under the conditions described above, gluino decays are expected to be dominated by the three-body process of Fig. 1a (1b). The gluino and LSP masses are treated as independent parameters.

It is rare for a T1bbbb event to contain an isolated high-p_{T} lepton. To define the search region for this study, we therefore veto events with an identified isolated electron or muon. We also veto events with an isolated charged track, characteristic of τ-lepton decay. The resulting collection of events is referred to as the zero-lepton (ZL) or "signal" sample. Besides the ZL sample, control samples are defined in order to evaluate the SM background. To evaluate the backgrounds from top-quark and W + jets events (where "top-quark" refers to both $\mathrm{t\bar{t}}$ and single-top-quark events), we select a top-quark- and W + jets-dominated control sample by requiring the presence of exactly one identified isolated electron or muon. We refer to this sample as the single-lepton (SL) sample. (Top-quark and W + jets events are grouped into a single background category because of their similar experimental signatures.) To evaluate the QCD multijet background, we employ the minimum normalized azimuthal angle $\Delta\hat{\phi}_{\mathrm{min}}$ [23] between the $E_{\mathrm{T}}^{\mathrm{miss}}$ vector and one of the three highest-p_{T} jets, selecting a QCD-dominated control sample by requiring small values of this variable.[1] We refer to this control sample as the low-$\Delta\hat{\phi}_{\mathrm{min}}$ (LDP) sample. The Z + jets background is evaluated with control samples of $\mathrm{Z} \to \ell^+\ell^-$ events ($\ell = \mathrm{e}$ and μ). Our analysis is performed in the framework of a global likelihood fit that simultaneously analyzes the signal and background content, accounting for signal contributions to the ZL and control samples in a unified and consistent manner.

In contrast to T1bbbb events, events in the T1tttt scenario are expected to appear in both the ZL and SL samples. Since our global likelihood fitting procedure can account for T1tttt contributions to the control samples, the analysis procedures and background evaluation methods used to examine the T1tttt scenario are essentially the same as those used for the T1bbbb scenario.

This study extends the analysis of Ref. [23] by exploiting the expected differences in shape between the T1bbbb or T1tttt scenario and each of the SM background components in the distributions of $E_{\mathrm{T}}^{\mathrm{miss}}$, the number $N_{\mathrm{b\text{-}jet}}$ of b-tagged jets in an event, and H_{T}, where H_{T} is the scalar sum of jet p_{T} values. (The quantitative definitions of $E_{\mathrm{T}}^{\mathrm{miss}}$ and H_{T} are given in Section 3.) The data are divided into mutually exclusive bins in these three variables, as indicated schematically in Fig. 2. The $E_{\mathrm{T}}^{\mathrm{miss}}$ and H_{T} distributions are divided into four bins each. The definitions of these bins are given in the table of Fig. 2. For the ZL, SL, and LDP samples, the b-jet multiplicity distribution is divided into three bins, corresponding to $N_{\mathrm{b\text{-}jet}} = 1$, 2, or $\geqslant 3$. There are 176 mutually exclusive bins of data in the analysis, 48 each for the ZL, SL, and LDP samples, and 16 each for the $\mathrm{Z} \to \mathrm{e^+e^-}$ and $\mathrm{Z} \to \mu^+\mu^-$ samples. The contents of the bins are examined simultaneously in the likelihood fit.

This Letter is organized as follows. In Section 2 we discuss the detector and trigger. Sections 3 and 4 describe the event selection. The likelihood framework and background determination methods are presented in Section 5. Section 6 presents the results and Section 7 a summary.

2. Detector and trigger

A detailed description of the CMS detector is given elsewhere [36]. The CMS coordinate system is defined with the origin at the center of the detector and the z axis along the direction of the counterclockwise beam. The transverse plane is perpendicular to the beam axis, with ϕ the azimuthal angle (measured in radians), θ the polar angle, and $\eta = -\ln[\tan(\theta/2)]$ the pseudo-rapidity. A superconducting solenoid provides an axial magnetic field of 3.8 T. Within the field volume are a silicon pixel and strip tracker, a crystal electromagnetic calorimeter, and a brass-scintillator hadron calorimeter. The tracking system is completed with muon detectors, based on gas-ionization chambers embedded in the steel flux-return yoke outside the solenoid. The tracking system covers $|\eta| < 2.5$ and the calorimeters $|\eta| < 3.0$. The $3 < |\eta| < 5$ region is instrumented with forward calorimeters. The near-hermeticity of the detector permits accurate measurements of energy balance in the transverse plane.

[1] For the current study, we use a slightly modified definition of the $\Delta\hat{\phi}_{\mathrm{min}}$ variable compared to Ref. [23]: we now use "arcsin" rather than "arctan" in the expression for $\sigma_{\Delta\phi,i}$ (see Section IV of Ref. [23]). This modification introduces a negligible difference for the small angles relevant here. Nonetheless, the modified expression is technically more correct than the original one.

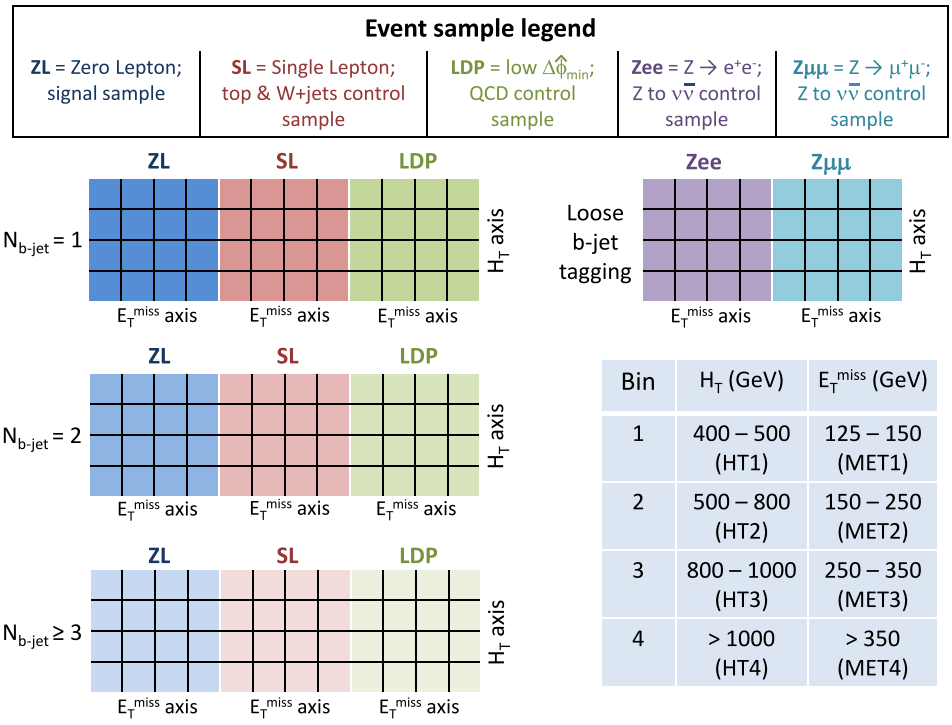

Bin	H_T (GeV)	E_T^{miss} (GeV)
1	400 – 500 (HT1)	125 – 150 (MET1)
2	500 – 800 (HT2)	150 – 250 (MET2)
3	800 – 1000 (HT3)	250 – 350 (MET3)
4	> 1000 (HT4)	> 350 (MET4)

Fig. 2. Schematic diagram illustrating the 176 mutually exclusive bins in the analysis. The E_T^{miss} and H_T distributions are divided into four bins each; the table gives the bin definitions. The designations HT*i* and MET*i* ($i = 1$–4) are used to label the individual H_T and E_T^{miss} bins. The $N_{b\text{-jet}}$ distributions of the signal sample (ZL), top-quark and W + jets control sample (SL), and QCD multijet control sample (LDP), contain three bins each, corresponding to exactly one, exactly two, and three or more identified b jets.

Events are selected using multiple trigger conditions, based primarily on thresholds for H_T and E_T^{miss}. The trigger efficiency, determined from data, is the probability for a signal or control sample event to satisfy the trigger conditions. In our analysis, the data are examined in exclusive regions of H_T and E_T^{miss}, as described above. The trigger is found to be nearly 100% efficient except in regions with low values of both H_T and E_T^{miss}. In the bin with lowest H_T and E_T^{miss}, i.e., the HT1–MET1 bin of Fig. 2, the evaluated trigger efficiency is 0.91 ± 0.01 (0.86 ± 0.09) for the trigger relevant for the ZL and SL (LDP) samples. Corrections are applied to account for the trigger efficiencies and their corresponding uncertainties.

3. Event selection

Physics objects are defined with the particle flow (PF) method [37], which is used to reconstruct and identify charged and neutral hadrons, electrons (with associated bremsstrahlung photons), muons, and photons, using an optimized combination of information from CMS subdetectors. Tau leptons are identified using the reconstructed PF objects. The event primary vertex is identified by selecting the reconstructed vertex that has the largest sum of charged-track p_T^2 values. Events are required to have a primary vertex with at least four charged tracks and that lies within 24 cm of the origin in the direction along the beam axis and 2 cm in the perpendicular direction. Charged particles used in the analysis must emanate from the primary vertex. In this way, charged particles associated with extraneous pp interactions within the same bunch crossing ("pileup") are disregarded. The PF objects serve as input for jet reconstruction, based on the anti-k_T algorithm [38] with a distance parameter of 0.5. Jet corrections are applied in both p_T and η to account for residual effects of non-uniform detector response. Additional corrections [39,40] account for pileup effects from neutral particles. The missing transverse energy E_T^{miss} is defined as the modulus of the vector sum of the transverse momenta of all PF objects. The E_T^{miss} vector is the negative of that same vector sum.

The requirements used to select the zero-lepton (ZL) event sample are as follows:

- at least three jets with $p_T > 50$ GeV and $|\eta| < 2.4$, where the two leading jets satisfy $p_T > 70$ GeV;
- $H_T > 400$ GeV, where H_T is calculated using jets with $p_T > 50$ GeV and $|\eta| < 2.4$;
- $E_T^{miss} > 125$ GeV;
- no identified, isolated electron or muon candidate with $p_T > 10$ GeV; electron candidates are restricted to $|\eta| < 2.5$ and muon candidates to $|\eta| < 2.4$;
- no isolated charged-particle track with $p_T > 15$ GeV and $|\eta| < 2.4$;
- $\Delta\hat{\phi}_{min} > 4.0$, where the $\Delta\hat{\phi}_{min}$ variable is described in Ref. [23];
- at least one b-tagged jet, where b-tagged jets are required to have $p_T > 50$ GeV and $|\eta| < 2.4$.

The isolated-track requirement eliminates events with an isolated electron or muon in cases where the lepton is not identified, as well as events with a τ lepton that decays hadronically. Electrons, muons, and tracks are considered isolated if the scalar sum of the p_T values of charged hadrons (for electrons and muons, also photons and neutral hadrons) surrounding the lepton or track within a cone of radius $\sqrt{(\Delta\eta)^2 + (\Delta\phi)^2} = 0.3$ (0.4 for muons), divided by the lepton or track p_T value itself, is less than 0.15, 0.20, and 0.05, respectively.

Identification of b jets is based on the combined-secondary-vertex algorithm described in Ref. [41] (we use the "medium" working point). This algorithm combines information about secondary vertices, track impact parameters, and jet kinematics, to separate b jets from light-flavored-quark, charm-quark, and gluon

jets. The nominal b-tagging efficiency is 75% for jets with a p_T value of 80 GeV, as determined from a sample of simulated b-jet-enriched events [41]. The corresponding misidentification rate for light-quark jets is 1.0%.

4. Control samples, search regions, and event simulation

The top-quark- and W + jets-dominated SL control sample is defined by selecting events with exactly one electron or one muon, using the lepton selection criteria and all other nominal selection requirements given in Section 3, with the exception of the requirement that there be no isolated track. To reduce potential contributions from signal T1tttt events, we apply an additional requirement $m_T < 100$ GeV to the SL sample only, where $m_T = \{2E_T^{\text{miss}} p_T^{\ell}[1 - \cos(\Delta\phi_{\ell, E_T^{\text{miss}}})]\}^{1/2}$ is the transverse mass formed from the E_T^{miss} and p_T^{ℓ} (lepton transverse momentum) vectors, with $\Delta\phi_{\ell, E_T^{\text{miss}}}$ the corresponding difference in the azimuthal angle.

The region $\Delta\hat{\phi}_{\text{min}} < 4$, with all other nominal selection requirements from Section 3 imposed, defines the QCD-dominated LDP control region.

To evaluate the Z + jets background, we select Z + jets control samples with $Z \to e^+e^-$ and $Z \to \mu^+\mu^-$ decays, as described in Section 5.3.

The data are divided into mutually exclusive bins of E_T^{miss}, H_T, and $N_{\text{b-jet}}$, as shown in Fig. 2. This binning is chosen based on simulation studies with SUSY signal and SM background event samples, for which signal sensitivity in the presence of SUSY events, and limits in the absence of such events, are both considered. The best performance is obtained with relatively narrow bins at low H_T and E_T^{miss}, which help to characterize the background shapes, and with multiple bins at high H_T and E_T^{miss}, which provide regions with reasonable signal efficiency and very little background. Within this general framework, the sensitivity is found to be relatively independent of particular binning choices.

To illustrate the characteristics of the events, Fig. 3 presents the distribution of $N_{\text{b-jet}}$ for the signal (ZL) and control-region (SL, LDP) samples, and the corresponding distributions of E_T^{miss} and H_T for $N_{\text{b-jet}} \geqslant 3$. The results are shown in comparison with Monte Carlo (MC) simulations of SM processes. The $t\bar{t}$, W + jets, and Z + jets MC samples are simulated at the parton level with the MadGraph 5.1.1.0 [42] event generator. Single-top-quark events are produced with the powheg 301 [43] program. The pythia 6.4.22 [44] generator is used for diboson and QCD multijet events. For all SM MC samples, the Geant4 [45] package is used to model the detector. The top-quark MC distributions are normalized to an approximate next-to-next-to-leading order (NNLO) cross-section calculation [46,47] and the simulated W + jets and Z + jets results to the inclusive NNLO cross sections from the fewz generator [48]. The diboson MC distribution, given by the sum of contributions from WW, WZ, and ZZ events, is normalized to NLO using the cross section from the mcfm generator [49]. The QCD multijet distribution is normalized to leading order. We also consider Drell–Yan events, generated with MadGraph and normalized to NNLO [48]. The contribution of Drell–Yan events is found to be small (at most one fifth the contribution of diboson events in all signal regions) and is not included in Fig. 3.

In general, the simulation is seen to agree with the data, although some features exhibit differences on the order of 20%. Note that these MC results are not used in the analysis but merely provide guidance on the expected background composition.

Signal T1bbbb and T1tttt MC samples are generated for a range of gluino $m_{\tilde{g}}$ and LSP $m_{\tilde{\chi}_1^0}$ mass values, with $m_{\tilde{\chi}_1^0} < m_{\tilde{g}}$. The signal samples are based on MadGraph, with up to two partons present in addition to the gluino pair. The decays of the gluino are described using a pure phase-space matrix element in pythia. To reduce computational requirements, the detector is modeled with the CMS fast simulation program [50,51], with corrections to account for modest differences observed with respect to the Geant4 simulation. Fig. 3 includes the distributions of two representative T1bbbb scenarios, one with $(m_{\tilde{g}}, m_{\tilde{\chi}_1^0}) = (600\ \text{GeV}, 500\ \text{GeV})$ and the other with $(m_{\tilde{g}}, m_{\tilde{\chi}_1^0}) = (1225\ \text{GeV}, 150\ \text{GeV})$, both of which are at the limit of our expected sensitivity (Section 6).

All MC samples incorporate the CTEQ6.6 [52,53] parton distribution functions, with pythia used to describe parton showering and hadronization. The MC distributions account for pileup interactions, as observed in data. In addition, we correct the simulation so that the b-tagging and misidentification efficiencies match those determined from control samples in the data. The b-tagging efficiency correction factor depends slightly on jet p_T and has a typical value of 0.95 [41]. A further correction, applied to the signal samples, accounts for mismodeling of initial-state radiation (ISR) in MadGraph. The correction is derived by comparing the p_T spectra of reconstructed Z bosons, $t\bar{t}$ pairs, and WZ pairs between data and simulation. At high values of transverse momentum of these systems, where the p_T is balanced by radiated jets, the MadGraph simulation is found to overestimate the observed event rate. The corresponding correction is negligible except for small values of the gluino–LSP mass difference where it can be as large as 20% for both the T1bbbb and T1tttt samples.

5. Likelihood function and background evaluation methods

In this section, we present the definition of the likelihood function and describe the background evaluation methods. We use the following notation:

- ZL: the zero-lepton event sample;
- SL: the single-lepton event sample;
- LDP: the low-$\Delta\hat{\phi}_{\text{min}}$ event sample;
- Zee and Z$\mu\mu$: the $Z \to e^+e^-$ and $Z \to \mu^+\mu^-$ event samples;
- ttWj: the top-quark and W + jets background component, where "top-quark" includes both $t\bar{t}$ and single-top-quark events;
- QCD: the QCD multijet background component;
- Z$\nu\nu$: the Z + jets (where $Z \to \nu\bar{\nu}$) background component;
- SUSY: the signal component;
- $\mu^{\text{C}}_{\text{S};i,j,k}$: the estimated number of events in bin i, j, k of event sample S for component C without accounting for trigger efficiency, where i, j, and k denote the bin in E_T^{miss}, H_T, and $N_{\text{b-jet}}$, respectively, and C denotes ttWj, QCD, or one of the other signal or background terms;
- $n_{\text{S};i,j,k}$: the estimated number of events in bin i, j, k of event sample S from all components after accounting for trigger efficiency;
- $\epsilon^{\text{trig}}_{\text{S};i,j,k}$: the trigger efficiency in bin i, j, k for event sample S;
- $N_{\text{S};i,j,k}$: the observed number of events in bin i, j, k for event sample S.

5.1. Top-quark and W + jets background

The SL sample is used to describe the shape of the top-quark and W + jets background in the three analysis dimensions of E_T^{miss}, H_T, and $N_{\text{b-jet}}$. The SL sample thus provides a three-dimensional (3D) binned probability density function (PDF) determined directly from data. The top-quark and W + jets background in each bin of the ZL sample is determined from this measured 3D shape, simulation-derived bin-by-bin corrections $S^{\text{ttWj}}_{i,j,k}$, and an overall

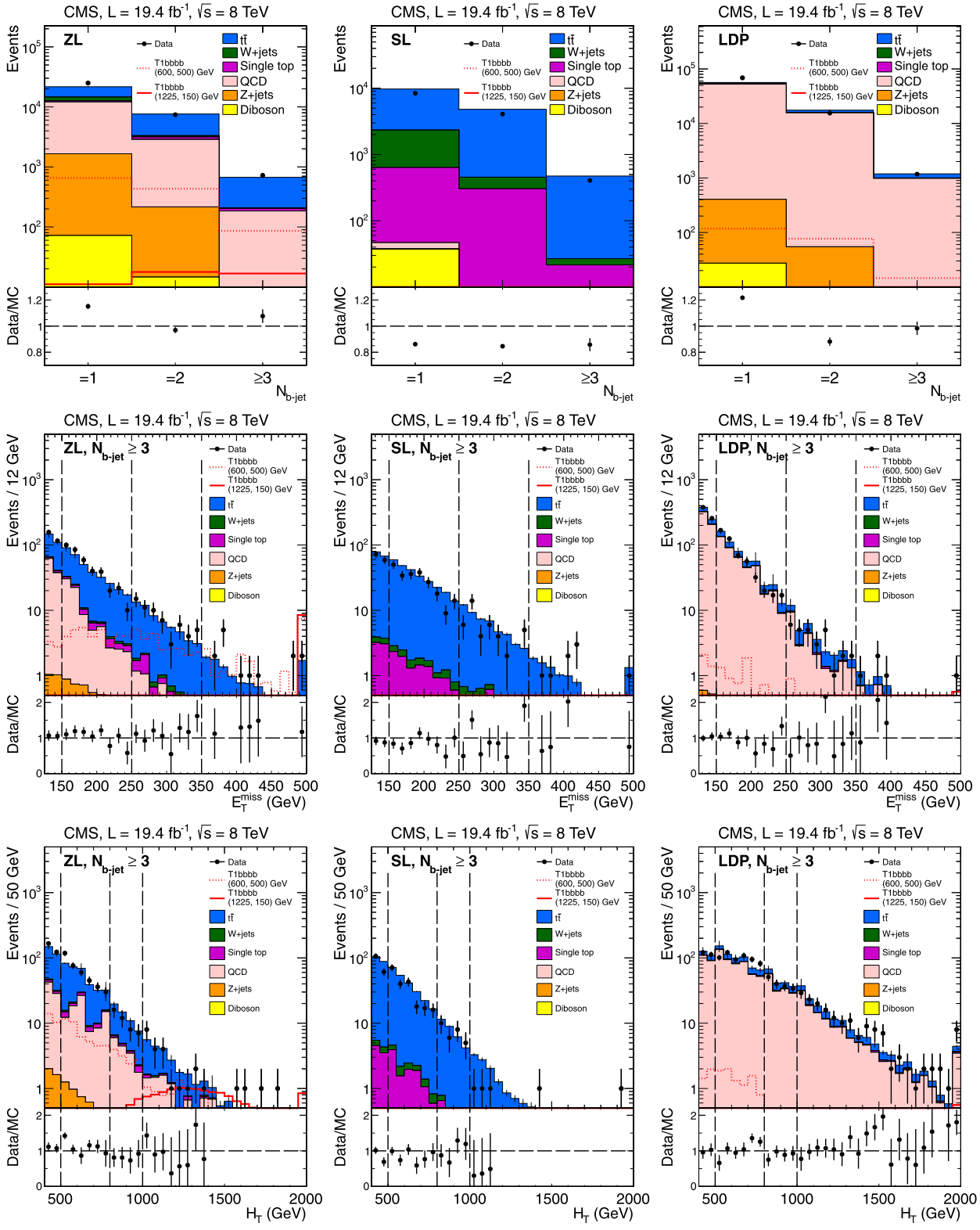

Fig. 3. [Top row] Data and Monte Carlo distributions of the number $N_{\text{b-jet}}$ of b-tagged jets for the [left column] signal (ZL) sample, [center column] top-quark and W+jets (SL) control sample, and [right column] QCD multijet (LDP) control sample. The lower panes show the ratio of the measured to the simulated events. [Center row] Corresponding $E_{\text{T}}^{\text{miss}}$ distributions, and [bottom row] H_{T} distributions, for events with $N_{\text{b-jet}} \geqslant 3$. The dashed vertical lines indicate the divisions between the four bins of $E_{\text{T}}^{\text{miss}}$ or H_{T}. Results for the T1bbbb scenario with $(m_{\tilde{g}}, m_{\tilde{\chi}_1^0}) = (600\ \text{GeV}, 500\ \text{GeV})$ and $(1225\ \text{GeV}, 150\ \text{GeV})$ are shown as unstacked distributions. For all results, the uncertainties are statistical only. The normalization of the simulated curves is based on the absolute cross sections, as described in the text.

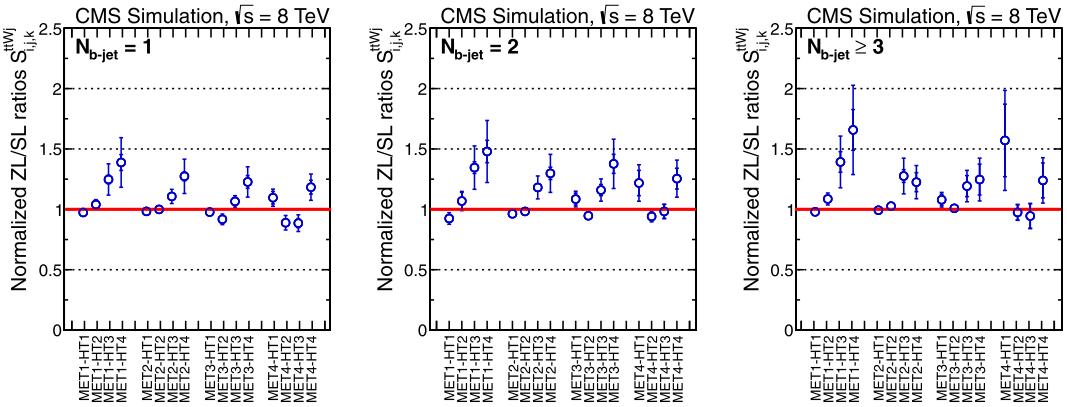

Fig. 4. [Left] Ratio of the number of events in the zero-lepton (ZL) sample to that in the single-lepton (SL) sample for simulated top-quark and W + jets events in the $16 H_T$–E_T^{miss} bins with $N_{b\text{-jet}} = 1$, divided by the average ratio value over the 64 bins with $N_{b\text{-jet}} = 1, 2,$ and $\geqslant 3$. The leftmost group of four consecutive points corresponds to E_T^{miss} bin 1 (MET1) of the table in Fig. 2, the next-leftmost group to E_T^{miss} bin 2 (MET2), etc. The four points within each group correspond to the four H_T bins in the table, increasing in H_T value from left to right (HT1 to HT4). The inner (outer) error bars show the statistical (combined statistical and systematic) uncertainties. [Center and right] The corresponding results for $N_{b\text{-jet}} = 2$ and $N_{b\text{-jet}} \geqslant 3$.

normalization term $R^{ttWj}_{ZL/SL}$ that is a free parameter in the fit, as described below.

With respect to SM processes, the SL sample is assumed to be populated by top-quark and W + jets events only. Contributions from QCD multijet and Z + jets events are small (around 1% on average) as seen from Fig. 3, and are accounted for with a systematic uncertainty. The contribution from T1bbbb events is negligible because isolated leptons are rare in the T1bbbb scenario. In contrast, with four top quarks in the final state, T1tttt events often contain an isolated high-p_T lepton, resulting in events that populate the SL sample. Therefore, we presume

$$n_{SL;i,j,k} = \epsilon^{trig}_{SL;i,j,k} \cdot \left(\mu^{ttWj}_{SL;i,j,k} + S^{SUSY}_{SL;i,j,k} \cdot \mu^{SUSY}_{SL;i,j,k}\right), \quad (1)$$

where $S^{SUSY}_{SL;i,j,k}$ is a nuisance parameter. For the T1bbbb scenario, $\mu^{SUSY}_{SL;i,j,k} = 0$.

We calculate the ratio of the number of top-quark and W + jets events in the ZL sample to the corresponding number in the SL sample, as predicted by simulation, after normalization to the same integrated luminosity. We consider the simulated ZL-to-SL ratios in three groups of 16 bins, one group corresponding to $N_{b\text{-jet}} = 1$, one to $N_{b\text{-jet}} = 2$, and one to $N_{b\text{-jet}} \geqslant 3$ (see Fig. 2). The 48 ratio values are each normalized by dividing by the average ratio value over the 48 bins. The resulting normalized ZL-to-SL ratios are shown in the left plot of Fig. 4 for $N_{b\text{-jet}} = 1$, in the center plot for $N_{b\text{-jet}} = 2$, and in the right plot for $N_{b\text{-jet}} \geqslant 3$. Were the 3D shape of top-quark and W + jets distributions the same in the simulated ZL and SL samples, all points in Fig. 4 would be consistent with unity. Deviations from unity on the order of 20–50% are seen for some points, indicating a shape difference between the two samples. The shape difference is strongest in the H_T dimension. This H_T dependence is due to the lepton isolation requirement, which is less likely to be satisfied as H_T increases. Consistent results are found if the POWHEG or MC@NLO [54] generator, rather than MADGRAPH, is used to produce the $t\bar{t}$ MC sample.

Our estimate of the top-quark and W + jets contribution to bin i, j, k of the ZL sample is thus

$$\mu^{ttWj}_{ZL;i,j,k} = S^{ttWj}_{i,j,k} \cdot R^{ttWj}_{ZL/SL} \cdot \mu^{ttWj}_{SL;i,j,k}, \quad (2)$$

where $R^{ttWj}_{ZL/SL}$ is the scale factor common to all bins mentioned above and the $S^{ttWj}_{i,j,k}$ factors are the MC-based terms presented in Fig. 4, which account for the 3D shape differences between the ZL and SL samples. In the likelihood function, the $S^{ttWj}_{i,j,k}$ terms are treated as nuisance parameters whose values are determined in the fit, each constrained by a lognormal PDF. The median of the lognormal is the corresponding value shown in Fig. 4, while the geometric standard deviation is $\ln(1 + \sigma_{rel})$, with σ_{rel} the relative uncertainty of the corresponding $S^{ttWj}_{i,j,k}$ term, determined from the quadratic sum of its statistical uncertainty and one half the difference from unity. In addition, we vary the W + jets cross section by 100% [55]. The difference with respect to the standard result defines an uncertainty for a lognormal distribution that is applied as an additional constraint on the $S^{ttWj}_{i,j,k}$ terms. An analogous constraint is derived through variation of the single-top-quark cross section by 30% [56].

5.2. QCD multijet background

The QCD multijet background in each bin of the ZL sample, in the 3D space of E_T^{miss}, H_T, and $N_{b\text{-jet}}$, is determined from the number of events in the corresponding bin of the LDP sample, in conjunction with multiplicative scale factors described below. Before applying these scale factors, the contributions of top-quark and W + jets events are subtracted from the measured LDP results, as are the contributions of Z + jets events. The estimate of the top-quark and W + jets contribution to the LDP sample is determined from the data-derived top-quark and W + jets event yield in the ZL sample, found in the likelihood fit (Section 6) for the corresponding bin, multiplied by the MC ratio of LDP to ZL events for that bin, and analogously for the Z + jets contribution to the LDP sample (these subtractions are performed simultaneously with all other aspects of the fit). The uncertainty assigned to this subtraction procedure accounts for the total uncertainty of the respective ZL event yield, and for a 10% uncertainty associated with the simulated ratio, where the latter term corresponds to the average statistical uncertainty of the MC ratio values.

The top row of Fig. 5 shows the ratio between the number of QCD multijet events in the ZL sample to the corresponding number in the LDP sample, as predicted by simulation, after normalization to the same integrated luminosity. The results are shown for the 48 bins of the ZL and LDP samples. This ratio is seen to depend strongly on H_T. The dependence on E_T^{miss} and $N_{b\text{-jet}}$ is more moderate. We parameterize the E_T^{miss}, H_T, and $N_{b\text{-jet}}$ dependence assuming that this dependence factorizes, i.e., we assume that the H_T dependence is independent of E_T^{miss} and $N_{b\text{-jet}}$, etc. We thus

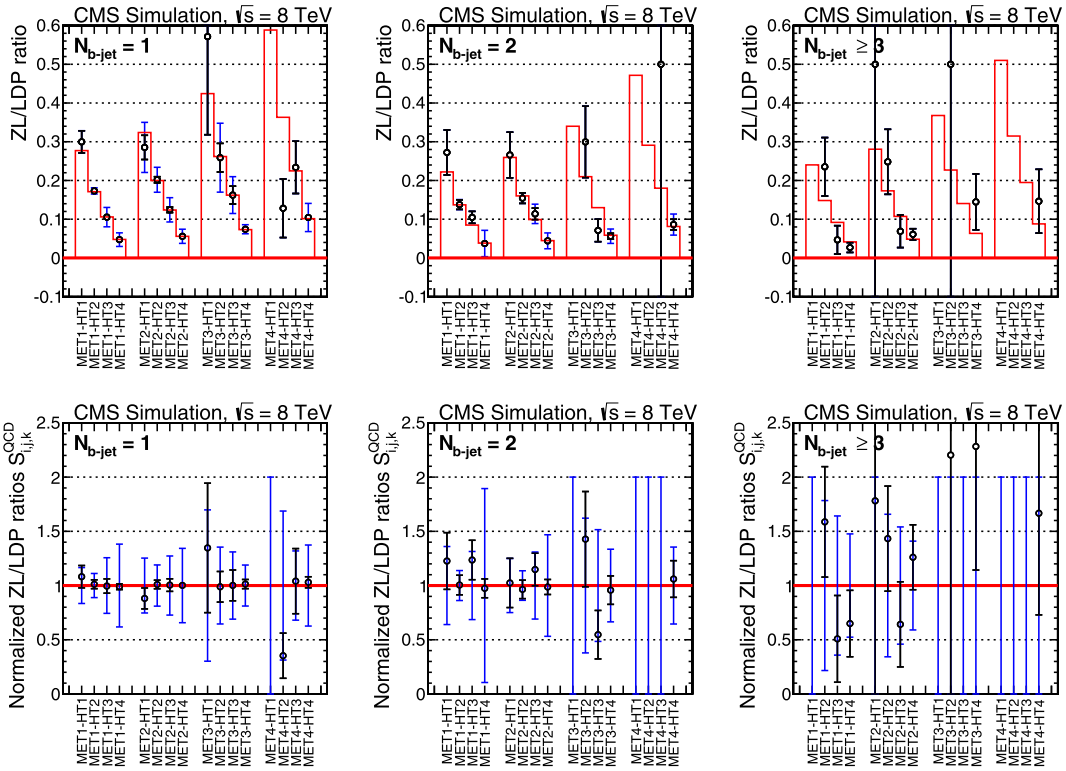

Fig. 5. [Top row] Ratio of the number of events in the zero-lepton (ZL) sample to that in the low-$\Delta\hat{\phi}_{\min}$ (LDP) sample for simulated QCD multijet events. The definitions of the bins are the same as in Fig. 4. Various QCD multijet samples, with different choices for the hardness scale ($\hat{p}_{\mathrm{T}}$ [44]) of the interaction, are combined. The points show the averages over those samples. The inner error bars indicate the statistical uncertainties. The outer error bars indicate the statistical uncertainties added in quadrature with the root-mean-squared values over the different $\hat{p}_{\mathrm{T}}$ samples. The histogram shows the results of the fitted parameterization described in the text. [Bottom row] The corresponding ratio divided by the parameterization from the top row. The inner (black) and outer (blue) error bars indicate the statistical and combined statistical-and-systematic uncertainties, respectively.

model the QCD multijet background contribution to the ZL sample for a given $E_{\mathrm{T}}^{\mathrm{miss}}$, H_{T}, $N_{\text{b-jet}}$ bin as:

$$\mu^{\mathrm{QCD}}_{\mathrm{ZL};i,j,k} = S^{\mathrm{QCD}}_{i,j,k} \cdot \left(K^{\mathrm{QCD}}_{\mathrm{MET},i} \cdot K^{\mathrm{QCD}}_{\mathrm{HT},j} \cdot K^{\mathrm{QCD}}_{\mathrm{Nb},k}\right) \cdot \mu^{\mathrm{QCD}}_{\mathrm{LDP};i,j,k}, \tag{3}$$

where the three K^{QCD} terms describe the $E_{\mathrm{T}}^{\mathrm{miss}}$, H_{T}, and $N_{\text{b-jet}}$ dependence and the $S^{\mathrm{QCD}}_{i,j,k}$ factors (defined below) are corrections to account for potential inadequacies in the parametrization. Note that some bins in the top row of Fig. 5 do not contain any entries. These bins generally have large $E_{\mathrm{T}}^{\mathrm{miss}}$ and small H_{T} values, making them kinematically unlikely (a large $E_{\mathrm{T}}^{\mathrm{miss}}$ value implies a large H_{T} value), and thus contain few or no events.

We fit the parameterization of Eq. (3) to the ratio values shown in the top row of Fig. 5, taking $S^{\mathrm{QCD}}_{i,j,k} \equiv 1$ at this stage, to determine simulation-derived values for the K^{QCD} factors (for the final results, most K^{QCD} factors are determined in the likelihood fit, as explained below). The results of this fit are shown by the histograms in the top row of Fig. 5. The simulated QCD ZL-to-LDP ratios divided by the fitted parameterization are shown in the bottom row of Fig. 5. The points in the bottom row are consistent with unity, indicating that the empirical parameterization of Eq. (3) is sufficient. Therefore, in the likelihood fit, no corrections to the parametrization are applied. The $S^{\mathrm{QCD}}_{i,j,k}$ factors are treated as nuisance parameters constrained by lognormal PDFs with a median set to unity. Geometric standard deviations for the lognormal distributions are set equal to the outer error bars in the bottom row of Fig. 5, given by the quadratic sum of the deviation of the ratios in the bottom row of Fig. 5 from unity, the statistical uncertainties of these ratios, and the root-mean-squared values found using the different QCD multijet samples described in Fig. 5 caption. For bins in the top row of Fig. 5 without any MC entries, we assign 100% uncertainties, which are indicated in the bottom row of the figure.

In the likelihood analysis, most of the K^{QCD} factors are free parameters in the fit: there is enough shape information that they can be determined directly from the data. However, we find from studies with simulation that the fit is unable to determine $K^{\mathrm{QCD}}_{\mathrm{MET},3}$, $K^{\mathrm{QCD}}_{\mathrm{MET},4}$, or $K^{\mathrm{QCD}}_{\mathrm{Nb},3}$. Instead, lognormal constraints are applied for these three parameters. The median values are set to the corresponding results from simulation and the geometric standard deviations to half the differences $K^{\mathrm{QCD}}_{\mathrm{MET},3} - K^{\mathrm{QCD}}_{\mathrm{MET},2}$, $K^{\mathrm{QCD}}_{\mathrm{MET},4} - K^{\mathrm{QCD}}_{\mathrm{MET},2}$, and $K^{\mathrm{QCD}}_{\mathrm{Nb},3} - K^{\mathrm{QCD}}_{\mathrm{Nb},1}$, respectively. The results of the fit are found to be insensitive to the choice of the geometric standard deviation values.

5.3. *The* Z + *jets background*

The Z + jets background (where $\mathrm{Z} \to \nu\bar{\nu}$) is evaluated by reconstructing $\mathrm{Z} \to \ell^+\ell^-$ events ($\ell = \mathrm{e}$ and μ). The ℓ^+ and ℓ^- leptons are then removed so that the events emulate Z + jets events with $\mathrm{Z} \to \nu\bar{\nu}$. The $\mathrm{Z} \to \mathrm{e}^+\mathrm{e}^-$ and $\mathrm{Z} \to \mu^+\mu^-$ samples are divided into 16 bins in the two-dimensional space of $E_{\mathrm{T}}^{\mathrm{miss}}$ and H_{T}, as indicated in Fig. 2.

Fits to the dilepton invariant mass spectra are performed to determine the $\mathrm{Z} \to \ell^+\ell^-$ yields. The yields are corrected to account for background, acceptance, and detection efficiency. The acceptance, determined from simulation, accounts for the larger fiducial volume for the detection of $\mathrm{Z} \to \nu\bar{\nu}$ events compared to $\mathrm{Z} \to \ell^+\ell^-$ events. The efficiency is $\epsilon = \epsilon_{\mathrm{trig}} \cdot \epsilon^2_{\ell\mathrm{reco}} \cdot \epsilon^2_{\ell\mathrm{sel}}$, where the trigger ϵ_{trig}, lepton reconstruction $\epsilon_{\ell\mathrm{reco}}$, and lepton selection $\epsilon_{\ell\mathrm{sel}}$ factors are determined from data.

The $Z \to \ell^+\ell^-$ yields are small in some of the signal regions. To increase these yields, we select events with the requirements of Section 3 except with a significantly looser b-tagging definition. The yield in each bin of this sample is multiplied by an extrapolation factor given by the ratio of the sum of the $Z \to \ell^+\ell^-$ yields over all H_T and E_T^{miss} bins for events that satisfy the nominal b-tagging requirements to those that satisfy the loose requirements.

To establish whether the extrapolation factors themselves exhibit a dependence on H_T or E_T^{miss}, we construct a control sample identical to the LDP sample except with the loosened b-tagging definition. This sample is dominated by QCD multijet production, and is found to have a distribution for the output variable of the b-tagging algorithm similar to that of the $Z \to \ell^+\ell^-$ events. From this control sample, we find that the $N_{b\text{-jet}} = 1$ extrapolation factors exhibit a variation with E_T^{miss} up to 25%; we apply this variation as a correction to those factors. For $N_{b\text{-jet}} = 2$ and $N_{b\text{-jet}} \geqslant 3$, we find no variation within the uncertainties and do not apply a correction.

The Z + jets background in the $i = E_T^{miss}$, $j = H_T$ bin of the ZL sample with $N_{b\text{-jet}} = 1$ is related to the corresponding bin in the $Z \to e^+e^-$ and $Z \to \mu^+\mu^-$ control samples through

$$\mu^{Zee}_{Zee;i,j} = \left(\mu^{Z\nu\nu}_{ZL;i,j,1} \cdot S_{ee} \cdot A_{ee;i} \cdot \epsilon_{ee}\right)/(\mathcal{F}_{Z\nu\nu;1} \cdot R_B), \quad (4)$$

$$\mu^{Z\mu\mu}_{Z\mu\mu;i,j} = \left(\mu^{Z\nu\nu}_{ZL;i,j,1} \cdot S_{\mu\mu} \cdot A_{\mu\mu;i} \cdot \epsilon_{\mu\mu}\right)/(\mathcal{F}_{Z\nu\nu;1} \cdot R_B), \quad (5)$$

where $A_{\ell\ell;i}$ and $\epsilon_{\ell\ell}$ are the acceptances and efficiencies for the $Z \to \ell^+\ell^-$ samples, respectively, $S_{\ell\ell}$ is a scale factor to account for systematic uncertainties, $R_B = 5.95 \pm 0.02$ is the ratio of the $Z \to \nu\bar{\nu}$ and $Z \to \ell^+\ell^-$ branching fractions [57], and $\mathcal{F}_{Z\nu\nu;1}$ is the extrapolation factor that relates the $N_{b\text{-jet}} = 1$ selection efficiency to the efficiency of the loose b-tagging requirement. The estimates of the Z+jets background for $N_{b\text{-jet}} = 2$ and $N_{b\text{-jet}} \geqslant 3$ are given by the $N_{b\text{-jet}} = 1$ result through the ratio of b-tagging extrapolation factors:

$$\mu^{Z\nu\nu}_{ZL;i,j,k} = \mu^{Z\nu\nu}_{ZL;i,j,1} \cdot (\mathcal{F}_{Z\nu\nu;k}/\mathcal{F}_{Z\nu\nu;1}), \quad (6)$$

where k is the $N_{b\text{-jet}}$ bin index.

Systematic uncertainties are evaluated for the $Z \to \ell^+\ell^-$ purity, acceptance, and detection efficiency by considering their dependence on E_T^{miss} and H_T, and by varying the selection conditions. An additional uncertainty, based on a consistency test performed with simulation, accounts for the level of agreement between the predicted and correct $Z \to \nu\bar{\nu}$ event rates. Finally, systematic uncertainties are evaluated for the extrapolation factors by varying the loosened b-tagging definition and by assigning an uncertainty to account for the observed or potential variation with E_T^{miss} and H_T (for the $N_{b\text{-jet}} = 2$ and $N_{b\text{-jet}} \geqslant 3$ factors, the latter uncertainty is based on the level of statistical fluctuation). The total systematic uncertainty of the $Z \to \nu\bar{\nu}$ background estimate is 30% for $N_{b\text{-jet}} = 1$, 35% for $N_{b\text{-jet}} = 2$, and 60% for $N_{b\text{-jet}} \geqslant 3$.

5.4. Other backgrounds

Backgrounds from diboson and Drell–Yan processes are accounted for using simulation, with an uncertainty of 100%. Their total fractional contribution to the overall background is 1% or less in all search regions.

5.5. Systematic uncertainties

Systematic uncertainties associated with the signal efficiency arise from various sources. A systematic uncertainty associated with the jet energy scale is evaluated by varying this scale by its p_T- and η-dependent uncertainties. The size of this uncertainty depends on the event kinematics, i.e., the E_T^{miss} bin, the H_T bin, and the assumed values of the gluino and LSP masses: typical values are in the range of 5–10%. A systematic uncertainty of 1% is associated with unclustered energy. This uncertainty is evaluated by varying the transverse energy in an event not clustered into a physics object by 10%. A systematic uncertainty of 3% is associated with anomalous E_T^{miss} values, caused by events that are misreconstructed or that contain beam-related background. This uncertainty is defined by 100% of the change in efficiency when software filters are applied to reject these events. The uncertainty of the luminosity determination is 4.4% [58]. The systematic uncertainties associated with corrections to the jet energy resolution, the pileup modeling mentioned in Section 3, the trigger efficiency, the b-tagging efficiency scale factor, and the ISR modeling are evaluated by varying the respective quantities by their uncertainties, while systematic uncertainties associated with the parton distribution functions are evaluated [52,59,60] following the recommendations of Ref. [61]. The jet energy resolution and pileup modeling uncertainties are 2% and 3%, respectively. The uncertainty of the trigger efficiency is generally below 2%. Uncertainties associated with the parton distribution functions and b-tagging efficiency are typically below 10% and 15%, respectively. The uncertainties of the T1bbbb (T1tttt) ISR modeling corrections are typically 5% (3%), but can be as large as 20% (20%) near the $m_{\tilde{g}} = m_{\tilde{\chi}^0_1}$ diagonal. The uncertainties associated with the jet energy scale, b-tagging efficiency, ISR modeling, and parton distribution functions vary significantly with the event kinematics and are evaluated point-by-point in the scans over gluino and LSP masses discussed in Section 6.

Systematic uncertainties for the SM background estimates are described in the previous sections. Note that, for our analysis, systematic uncertainties are generally much smaller than statistical uncertainties, where the latter terms primarily arise as a consequence of the limited numbers of events in the data control samples.

5.6. The global likelihood function

The likelihood function is the product of Poisson PDFs, one for each bin, and the constraint PDFs for the nuisance parameters. For each bin, the Poisson PDF gives the probability to observe N events, given a mean n, where n depends on the parameters of the likelihood model such as those given in Eqs. (1)–(6). The region with $E_T^{miss} > 350$ GeV and $400 < H_T < 500$ GeV, representing the bin with highest E_T^{miss} and lowest H_T in our analysis (the HT1–MET4 bin of Fig. 2), is at an extreme limit of phase space and is very sparsely populated, making it difficult to validate the background evaluation procedures. Furthermore, very few signal events are expected in this region. We therefore exclude the HT1–MET4 bin from the likelihood analysis, corresponding to 11 of the 176 bins. Thus, the effective number of bins in the analysis is 165.

For both signal and background terms, external input parameters are allowed to vary and are constrained by a PDF in the likelihood. Parameters with values between zero and one, such as efficiencies, are constrained by beta-distribution PDFs (see Section 35 of Ref. [57]). All others are constrained by lognormal PDFs. Correlations between the different kinematic regions, including the $N_{b\text{-jet}}$ bins, are taken into account. The test statistic is $q_\mu = -2\ln(\mathcal{L}_\mu/\mathcal{L}_{max})$, where $\mathcal{L}_{max}$ is the maximum likelihood determined by allowing all parameters including the SUSY signal strength μ to vary, and $\mathcal{L}_\mu$ is the maximum likelihood for a fixed signal strength.

Table 1
Observed numbers of events, SM background estimates from the fit, and SM expectations from Monte Carlo simulation, for the signal (ZL) regions with $E_{\mathrm{T}}^{\mathrm{miss}} > 350$ GeV and $N_{\mathrm{b\text{-}jet}} = 2$. The labels HT2, HT3, and HT4 refer to the bins of H_{T} indicated in Fig. 2, while HT2–4 is the sum over the three bins. The fourth row presents the SM background estimates from the sideband fit described in the text. The uncertainties listed for the fit results include the statistical and systematic components, while those shown for the simulation are statistical only. For the fits, the SUSY signal strength is fixed to zero. The last row shows the expected numbers of events from a SUSY test scenario described in the text.

$N_{\mathrm{b\text{-}jet}} = 2$, MET4	HT2	HT3	HT4	HT2–4
Observed number of events	66	19	19	104
SM background estimates from fit	$70.5^{+6.3}_{-5.9}$	$20.7^{+3.2}_{-2.8}$	$19.0^{+3.2}_{-2.8}$	110 ± 8
SM background predictions from simulation	81.6 ± 1.9	28.7 ± 1.3	23.3 ± 0.8	134 ± 2
SM background estimates from sideband fit	$76.4^{+10.2}_{-9.1}$	$22.3^{+4.5}_{-3.9}$	$19.0^{+4.5}_{-3.7}$	118^{+13}_{-12}
Number of signal events, SUSY test scenario	0.5	1.5	11.6	13.6

Table 2
Observed numbers of events, SM background estimates from the fit, and SM expectations from Monte Carlo simulation, for the signal (ZL) regions with $E_{\mathrm{T}}^{\mathrm{miss}} > 150$ GeV and $N_{\mathrm{b\text{-}jet}} \geqslant 3$. The labels HT1, HT2, MET2, etc., refer to the bins of H_{T} and $E_{\mathrm{T}}^{\mathrm{miss}}$ indicated in Fig. 2, while HT1–4 (MET2–4) is the sum over the four H_{T} (three $E_{\mathrm{T}}^{\mathrm{miss}}$) bins. The HT1–MET4 bin is excluded from the analysis, as explained in the text. The fourth section presents the SM background estimates from the sideband fit described in the text. The uncertainties listed for the fit results include the statistical and systematic components, while those shown for the simulation are statistical only. For the fits, the SUSY signal strength is fixed to zero. The last section shows the expected numbers of events from a SUSY test scenario described in the text.

$N_{\mathrm{b\text{-}jet}} \geqslant 3$	HT1	HT2	HT3	HT4	HT1–4
Observed number of events					
MET2	161	182	18	14	375
MET3	15	36	6	4	61
MET4	–	8	2	4	14
MET2–4	176	226	26	22	450
SM background estimates from fit					
MET2	157^{+13}_{-12}	179^{+13}_{-12}	$23.2^{+3.8}_{-3.4}$	$12.3^{+2.7}_{-2.3}$	372^{+19}_{-18}
MET3	$15.5^{+3.0}_{-2.6}$	$32.1^{+4.3}_{-3.8}$	$5.9^{+1.9}_{-1.5}$	$2.9^{+1.3}_{-1.0}$	$56.5^{+5.7}_{-5.4}$
MET4	–	$8.4^{+2.1}_{-1.8}$	$2.0^{+1.0}_{-0.7}$	$2.1^{+1.1}_{-0.9}$	$12.4^{+2.5}_{-2.2}$
MET2–4	173^{+13}_{-12}	220^{+14}_{-13}	$31.0^{+4.3}_{-3.8}$	$17.3^{+3.1}_{-2.8}$	441^{+20}_{-19}
SM background predictions from simulation					
MET2	127 ± 8	180 ± 12	27 ± 2	13 ± 1	347 ± 14
MET3	14.7 ± 0.7	30.9 ± 0.7	7.5 ± 0.4	3.9 ± 0.2	56.9 ± 2.6
MET4	–	6.1 ± 0.2	2.6 ± 0.2	2.6 ± 0.2	11.3 ± 0.3
MET2–4	141 ± 8	217 ± 12	37 ± 2	20 ± 1	415 ± 15
SM background estimates from sideband fit					
MET2	119^{+32}_{-19}	158^{+36}_{-24}	$28.2^{+6.9}_{-5.7}$	$10.2^{+3.5}_{-2.7}$	316^{+49}_{-37}
MET3	$15.2^{+4.3}_{-3.5}$	$27.7^{+5.8}_{-4.9}$	$5.6^{+2.6}_{-1.9}$	$2.0^{+1.5}_{-0.9}$	$50.5^{+8.2}_{-7.3}$
MET4	–	$8.3^{+2.9}_{-2.2}$	$1.9^{+1.3}_{-0.8}$	$0.4^{+0.6}_{-0.2}$	$10.5^{+3.2}_{-2.5}$
MET2–4	134^{+32}_{-20}	194^{+36}_{-26}	$35.7^{+7.5}_{-6.3}$	$12.6^{+3.8}_{-3.0}$	377^{+51}_{-42}
Number of signal events, SUSY test scenario					
MET2	0.0	0.1	0.2	1.0	1.4
MET3	0.0	0.2	0.4	2.0	2.6
MET4	–	0.4	1.4	10.8	12.6
MET2–4	0.0	0.7	2.0	13.8	16.6

6. Results

SUSY events in the T1bbbb and T1tttt scenarios often contain significant $E_{\mathrm{T}}^{\mathrm{miss}}$ and multiple b jets, as discussed in the Introduction. Tables 1 and 2 and Fig. 6 present the results of the fit for the 14 bins of the analysis that we find to be most sensitive to these two scenarios: the three bins with $H_{\mathrm{T}} > 500$ GeV, $E_{\mathrm{T}}^{\mathrm{miss}} > 350$ GeV, and $N_{\mathrm{b\text{-}jet}} = 2$, for which the results are shown in Table 1, and the 11 bins with $E_{\mathrm{T}}^{\mathrm{miss}} > 150$ GeV and $N_{\mathrm{b\text{-}jet}} \geqslant 3$, for which the results are shown in Table 2. For these results, the SUSY signal strength is set to zero so that we can test the compatibility of the data with the SM hypothesis. For the scan results over gluino and LSP masses presented below, the SUSY signal strength is allowed to vary.

The top row of Table 1 and top section of Table 2 show the numbers of events observed in data. The second row and section show the SM background estimates obtained from the fit, which are seen to be in agreement with the data to within the uncertainties. The third row and section present the SM predictions from the simulation. The simulated results are for guidance only and are not used in the analysis.

It is also interesting to perform the likelihood fit with the Poisson PDF terms for the 14 "most sensitive" bins removed, in order to ascertain the data-derived SM background estimates when the data in these bins do not affect the result. We call such a fit the "sideband" fit, which is therefore based on 151 bins. The sideband fit results for the numbers of SM background events in the 14 bins are presented in the fourth row of Table 1 and section of Table 2. For the sideband fit, the deviations with respect to the data are seen to be somewhat larger than for the standard fit. The largest deviation between observation and SM expectation occurs for the bin with $N_{\mathrm{b\text{-}jet}} \geqslant 3$, $H_{\mathrm{T}} > 1000$ GeV, and $E_{\mathrm{T}}^{\mathrm{miss}} > 350$ GeV (the HT4–MET4 bin of Table 2), where 4 events are observed whereas only $0.4^{+0.6}_{-0.2}$ events are expected (note that these uncertainties are not Gaussian). From studies with ensembles of simulated experi-

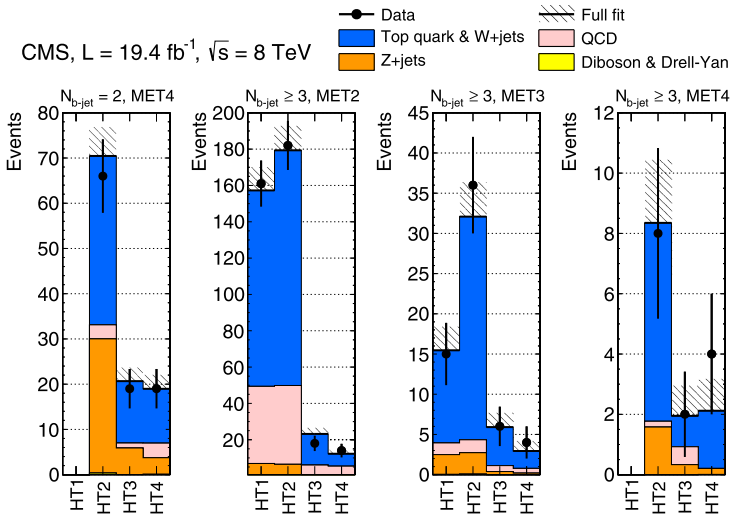

Fig. 6. Observed numbers of events (points with error bars) for the 14 bins with highest signal sensitivity in the analysis, in comparison with the standard model background predictions (with total uncertainties shown by the hatched bands) found in the fit with SUSY signal strength fixed to zero. The labels HT1, HT2, MET2, etc., refer to the bins of H_T and E_T^{miss} indicated in Fig. 2.

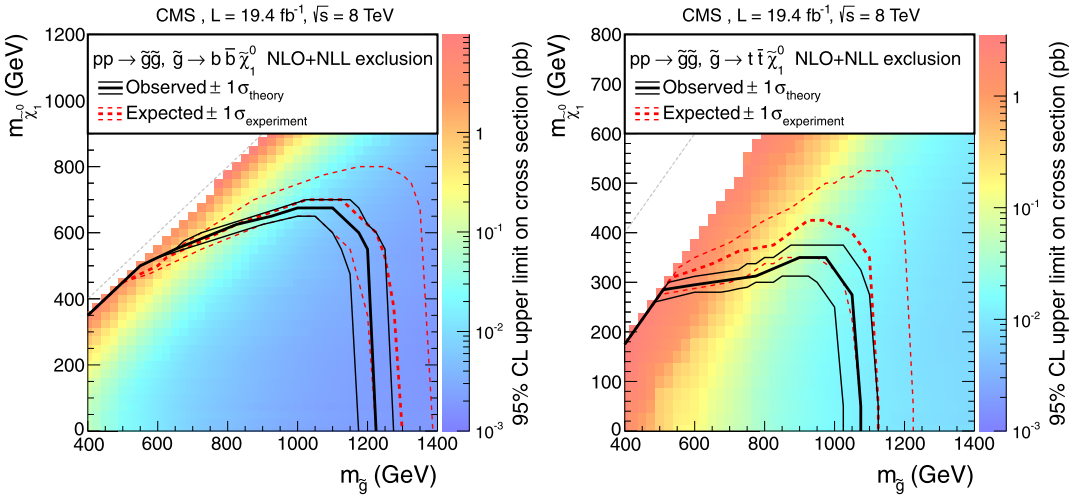

Fig. 7. The 95% CL upper limits on the [left] T1bbbb and [right] T1tttt new-physics scenario cross sections (pb) derived using the CL_s method. The solid (black) contours show the observed exclusions assuming the NLO + NLL cross sections [30–34], along with the ±1 standard deviation theory uncertainties [62]. The dashed (red) contours present the corresponding expected results, along with the ±1 standard deviation experimental uncertainties.

ments, considering only this bin, we estimate the probability for a fluctuation in the background in this bin to match or exceed 4 events to be 9% and do not consider this excess further.

For purposes of illustration, the last row of Table 1 and section of Table 2 show the expected numbers of signal events for a T1bbbb "test scenario" near the limit of our sensitivity, with $m_{\tilde{g}} = 1225$ GeV and $m_{\tilde{\chi}_1^0} = 150$ GeV.

Upper limits on the cross sections to produce events in the T1bbbb and T1tttt scenarios are determined at 95% confidence level (CL). The limits, based on the CL_s [63,64] technique with the test statistic q_μ defined above, are presented as a function of the gluino and LSP masses. Using the NLO+NLL cross section as a reference, we also evaluate the corresponding 95% CL exclusion curves. The results are shown in Fig. 7. The selection efficiency for T1bbbb (T1tttt) events is fairly constant at about 60% (25%) except for points to the left of a line parallel to the diagonal that intersects the $m_{\tilde{\chi}_1^0} = 0$ axis at around $m_{\tilde{g}} = 400$ GeV (550 GeV) or for gluino masses below about 550 GeV (680 GeV), where the efficiency decreases smoothly to 15% or less. Conservatively using the minus-one-standard-deviation result [62] for the reference cross sections, and in the limit of a massless LSP, we exclude gluinos with masses below 1170 GeV and 1020 GeV, respectively, in the T1bbbb and T1tttt scenarios. While these limits do not exclude the entire range of gluino masses $m_{\tilde{g}} \lesssim 1.5$ TeV suggested by natural models of SUSY [11], they are nonetheless among the most stringent bounds that have yet been obtained and greatly improve our results from Ref. [23].

7. Summary

A search is presented for an anomalous rate of events with three or more jets, at least one bottom-quark-tagged jet, no identified isolated electron or muon or isolated charged track, and large missing transverse energy. The search is based on a sample of proton–proton collision data collected at $\sqrt{s} = 8$ TeV with the CMS detector at the LHC in 2012, corresponding to an integrated luminosity of 19.4 fb^{-1}. The principal standard model backgrounds, from events with top quarks, W bosons and jets, Z bosons and jets, and QCD multijet production, are evaluated using control samples in the data. The analysis is performed in the framework of a

global likelihood fit in which the numbers of events in 165 exclusive bins in a three-dimensional array of missing transverse energy, the number of b-tagged jets, and the scalar sum of jet p_T values, are simultaneously examined. The standard model background estimates are found to agree with the observed numbers of events to within the uncertainties. We interpret the results in the context of simplified SUSY scenarios in which gluino pair production is followed by the decay of each gluino to an undetected particle and either a bottom or top quark–antiquark pair, characteristic of gluino mediated bottom- or top-squark production. Using the NLO + NLL production cross section as a reference, and in the limit of a massless lightest supersymmetric particle, we exclude gluinos with masses below 1170 GeV and 1020 GeV for the two scenarios, respectively. These are among the most stringent bounds that have yet been obtained for gluino mediated bottom and top squark production.

Acknowledgements

We congratulate our colleagues in the CERN accelerator departments for the excellent performance of the LHC and thank the technical and administrative staffs at CERN and at other CMS institutes for their contributions to the success of the CMS effort. In addition, we gratefully acknowledge the computing centres and personnel of the Worldwide LHC Computing Grid for delivering so effectively the computing infrastructure essential to our analyses. Finally, we acknowledge the enduring support for the construction and operation of the LHC and the CMS detector provided by the following funding agencies: BMWF and FWF (Austria); FNRS and FWO (Belgium); CNPq, CAPES, FAPERJ, and FAPESP (Brazil); MEYS (Bulgaria); CERN; CAS, MoST, and NSFC (China); COLCIENCIAS (Colombia); MSES (Croatia); RPF (Cyprus); MoER, SF0690030s09 and ERDF (Estonia); Academy of Finland, MEC, and HIP (Finland); CEA and CNRS/IN2P3 (France); BMBF, DFG, and HGF (Germany); GSRT (Greece); OTKA and NKTH (Hungary); DAE and DST (India); IPM (Iran); SFI (Ireland); INFN (Italy); NRF and WCU (Republic of Korea); LAS (Lithuania); CINVESTAV, CONACYT, SEP, and UASLP-FAI (Mexico); MSI (New Zealand); PAEC (Pakistan); MSHE and NSC (Poland); FCT (Portugal); JINR (Armenia, Belarus, Georgia, Ukraine, Uzbekistan); MON, RosAtom, RAS and RFBR (Russia); MSTD (Serbia); SEIDI and CPAN (Spain); Swiss Funding Agencies (Switzerland); NSC (Taipei); ThEPCenter, IPST and NSTDA (Thailand); TUBITAK and TAEK (Turkey); NASU (Ukraine); STFC (United Kingdom); DOE and NSF (USA).

Individuals have received support from the Marie-Curie programme and the European Research Council and EPLANET (European Union); the Leventis Foundation; the A.P. Sloan Foundation; the Alexander von Humboldt Foundation; the Belgian Federal Science Policy Office; the Fonds pour la Formation à la Recherche dans l'Industrie et dans l'Agriculture (FRIA-Belgium); the Agentschap voor Innovatie door Wetenschap en Technologie (IWT-Belgium); the Ministry of Education, Youth and Sports (MEYS) of Czech Republic; the Council of Science and Industrial Research, India; the Compagnia di San Paolo (Torino); the HOMING PLUS programme of Foundation for Polish Science, cofinanced by EU, Regional Development Fund; and the Thalis and Aristeia programmes cofinanced by EU-ESF and the Greek NSRF.

Open access

References

[1] P. Ramond, Dual theory for free fermions, Phys. Rev. D 3 (1971) 2415, http://dx.doi.org/10.1103/PhysRevD.3.2415.
[2] Y.A. Golfand, E.P. Likhtman, Extension of the algebra of Poincaré group generators and violation of P invariance, JETP Lett. 13 (1971) 323.
[3] A. Neveu, J.H. Schwarz, Factorizable dual model of pions, Nucl. Phys. B 31 (1971) 86, http://dx.doi.org/10.1016/0550-3213(71)90448-2.
[4] D.V. Volkov, V.P. Akulov, Possible universal neutrino interaction, JETP Lett. 16 (1972) 438.
[5] J. Wess, B. Zumino, A Lagrangian model invariant under supergauge transformations, Phys. Lett. B 49 (1974) 52, http://dx.doi.org/10.1016/0370-2693(74)90578-4.
[6] J. Wess, B. Zumino, Supergauge transformations in four dimensions, Nucl. Phys. B 70 (1974) 39, http://dx.doi.org/10.1016/0550-3213(74)90355-1.
[7] P. Fayet, Supergauge invariant extension of the Higgs mechanism and a model for the electron and its neutrino, Nucl. Phys. B 90 (1975) 104, http://dx.doi.org/10.1016/0550-3213(75)90636-7.
[8] H.P. Nilles, Supersymmetry, supergravity and particle physics, Phys. Rep. 110 (1984) 1, http://dx.doi.org/10.1016/0370-1573(84)90008-5.
[9] S. Dimopoulos, G.F. Giudice, Naturalness constraints in supersymmetric theories with nonuniversal soft terms, Phys. Lett. B 357 (1995) 573, http://dx.doi.org/10.1016/0370-2693(95)00961-J, arXiv:hep-ph/9507282.
[10] R. Barbieri, D. Pappadopulo, S-particles at their naturalness limits, JHEP 0910 (2009) 061, http://dx.doi.org/10.1088/1126-6708/2009/10/061, arXiv:0906.4546.
[11] M. Papucci, J.T. Ruderman, A. Weiler, Natural SUSY endures, JHEP 1209 (2012) 035, http://dx.doi.org/10.1007/JHEP09(2012)035, arXiv:1110.6926.
[12] G.R. Farrar, P. Fayet, Phenomenology of the production, decay, and detection of new hadronic states associated with supersymmetry, Phys. Lett. B 76 (1978) 575, http://dx.doi.org/10.1016/0370-2693(78)90858-4.
[13] ATLAS Collaboration, Search for supersymmetry in pp collisions at $\sqrt{s} = 7$ TeV in final states with missing transverse momentum and b jets, Phys. Lett. B 701 (2011) 398, http://dx.doi.org/10.1016/j.physletb.2011.06.015, arXiv:1103.4344.
[14] ATLAS Collaboration, Search for scalar bottom pair production with the ATLAS detector in pp collisions at $\sqrt{s} = 7$ TeV, Phys. Rev. Lett. 108 (2012) 181802, http://dx.doi.org/10.1103/PhysRevLett.108.181802, arXiv:1112.3832.
[15] ATLAS Collaboration, Search for supersymmetry in pp collisions at $\sqrt{s} = 7$ TeV in final states with missing transverse momentum and b jets with the ATLAS detector, Phys. Rev. D 85 (2012) 112006, http://dx.doi.org/10.1103/PhysRevD.85.112006, arXiv:1203.6193.
[16] ATLAS Collaboration, Search for top and bottom squarks from gluino pair production in final states with missing transverse energy and at least three b jets with the ATLAS detector, Eur. Phys. J. C 72 (2012) 2174, http://dx.doi.org/10.1140/epjc/s10052-012-2174-z, arXiv:1207.4686.
[17] ATLAS Collaboration, Search for a supersymmetric partner to the top quark in final states with jets and missing transverse momentum at $\sqrt{s} = 7$ TeV with the ATLAS detector, Phys. Rev. Lett. 109 (2012) 211802, http://dx.doi.org/10.1103/PhysRevLett.109.211802, arXiv:1208.1447.
[18] ATLAS Collaboration, Search for direct top squark pair production in final states with one isolated lepton, jets, and missing transverse momentum in $\sqrt{s} = 7$ TeV pp collisions using 4.7 fb^{-1} of ATLAS data, Phys. Rev. Lett. 109 (2012) 211803, http://dx.doi.org/10.1103/PhysRevLett.109.211803, arXiv:1208.2590.
[19] ATLAS Collaboration, Search for light top squark pair production in final states with leptons and b jets with the ATLAS detector in $\sqrt{s} = 7$ TeV proton–proton collisions, Phys. Lett. B 720 (2013) 13, http://dx.doi.org/10.1016/j.physletb.2013.01.049, arXiv:1209.2102.
[20] CMS Collaboration, Search for supersymmetry in events with b jets and missing transverse momentum at the LHC, JHEP 1107 (2011) 113, http://dx.doi.org/10.1007/JHEP07(2011)113, arXiv:1106.3272.
[21] CMS Collaboration, Search for new physics in events with same-sign dileptons and b-tagged jets in pp collisions at $\sqrt{s} = 7$ TeV, JHEP 1208 (2012) 110, http://dx.doi.org/10.1007/JHEP08(2012)110, arXiv:1205.3933.
[22] CMS Collaboration, Search for supersymmetry in hadronic final states using M_{T2} in pp collisions at $\sqrt{s} = 7$ TeV, JHEP 1210 (2012) 018, http://dx.doi.org/10.1007/JHEP10(2012)018, arXiv:1207.1798.
[23] CMS Collaboration, Search for supersymmetry in events with b-quark jets and missing transverse energy in pp collisions at 7 TeV, Phys. Rev. D 86 (2012) 072010, http://dx.doi.org/10.1103/PhysRevD.86.072010, arXiv:1208.4859.
[24] CMS Collaboration, Search for supersymmetry in final states with missing transverse energy and 0, 1, 2, or $\geqslant 3$ b-quark jets in 7 TeV pp collisions using the variable α_T, JHEP 1301 (2013) 077, http://dx.doi.org/10.1007/JHEP01(2013)077, arXiv:1210.8115.
[25] S. Chatrchyan, et al., CMS Collaboration, Search for supersymmetry in final states with a single lepton, b-quark jets, and missing transverse energy in proton–proton collisions at $\sqrt{s} = 7$ TeV, Phys. Rev. D 87 (2013) 052006, http://dx.doi.org/10.1103/PhysRevD.87.052006, arXiv:1211.3143.

[26] N. Arkani-Hamed, P. Schuster, N. Toro, J. Thaler, L.-T. Wang, B. Knuteson, S. Mrenna, MARMOSET: The path from LHC data to the new standard model via on-shell effective theories, arXiv:hep-ph/0703088, 2007.
[27] J. Alwall, P. Schuster, N. Toro, Simplified models for a first characterization of new physics at the LHC, Phys. Rev. D 79 (2009) 075020, http://dx.doi.org/10.1103/PhysRevD.79.075020, arXiv:0810.3921.
[28] J. Alwall, M.-P. Le, M. Lisanti, J.G. Wacker, Model-independent jets plus missing energy searches, Phys. Rev. D 79 (2009) 015005, http://dx.doi.org/10.1103/PhysRevD.79.015005, arXiv:0809.3264.
[29] D. Alves, N. Arkani-Hamed, S. Arora, Y. Bai, M. Baumgart, J. Berger, M. Buckley, B. Butler, S. Chang, H.-C. Cheng, C. Cheung, R.S. Chivukula, W.S. Cho, R. Cotta, M. D'Alfonso, et al., Simplified models for LHC new physics searches, J. Phys. G 39 (2012) 105005, http://dx.doi.org/10.1088/0954-3899/39/10/105005, arXiv:1105.2838.
[30] W. Beenakker, R. Höpker, M. Spira, P.M. Zerwas, Squark and gluino production at hadron colliders, Nucl. Phys. B 492 (1997) 51, http://dx.doi.org/10.1016/S0550-3213(97)00084-9, arXiv:hep-ph/9610490.
[31] A. Kulesza, L. Motyka, Threshold resummation for squark–antisquark and gluino-pair production at the LHC, Phys. Rev. Lett. 102 (2009) 111802, http://dx.doi.org/10.1103/PhysRevLett.102.111802, arXiv:0807.2405.
[32] A. Kulesza, L. Motyka, Soft gluon resummation for the production of gluino–gluino and squark–antisquark pairs at the LHC, Phys. Rev. D 80 (2009) 095004, http://dx.doi.org/10.1103/PhysRevD.80.095004, arXiv:0905.4749.
[33] W. Beenakker, S. Brensing, M. Krämer, A. Kulesza, E. Laenen, I. Niessen, Soft-gluon resummation for squark and gluino hadroproduction, JHEP 0912 (2009) 041, http://dx.doi.org/10.1088/1126-6708/2009/12/041, arXiv:0909.4418.
[34] W. Beenakker, S. Brensing, M. Krämer, A. Kulesza, E. Laenen, L. Motyka, I. Niessen, Squark and gluino hadroproduction, Int. J. Mod. Phys. A 26 (2011) 2637, http://dx.doi.org/10.1142/S0217751X11053560, arXiv:1105.1110.
[35] CMS Collaboration, Interpretation of searches for supersymmetry with simplified models, Phys. Rev. D (2013), in press, arXiv:1301.2175.
[36] CMS Collaboration, The CMS experiment at the CERN LHC, JINST 3 (2008) S08004, http://dx.doi.org/10.1088/1748-0221/3/08/S08004.
[37] CMS Collaboration, Particle flow event reconstruction in CMS and performance for jets, taus and $E_{\mathrm{T}}^{\mathrm{miss}}$, CMS Physics Analysis Summary CMS-PAS-PFT-09-001, http://cdsweb.cern.ch/record/1194487, 2009.
[38] M. Cacciari, G.P. Salam, G. Soyez, The anti-k_t jet clustering algorithm, JHEP 0804 (2008) 063, http://dx.doi.org/10.1088/1126-6708/2008/04/063, arXiv:0802.1189.
[39] CMS Collaboration, Determination of jet energy calibration and transverse momentum resolution in CMS, JINST 6 (2011) P11002, http://dx.doi.org/10.1088/1748-0221/6/11/P11002, arXiv:1107.4277.
[40] M. Cacciari, G.P. Salam, G. Soyez, FastJet user manual, Eur. Phys. J. C 72 (2012) 1896, http://dx.doi.org/10.1140/epjc/s10052-012-1896-2, arXiv:1111.6097.
[41] CMS Collaboration, Identification of b-quark jets with the CMS experiment, JINST 8 (2013) P04013, http://dx.doi.org/10.1088/1748-0221/8/04/P04013, arXiv:1211.4462.
[42] J. Alwall, M. Herquet, F. Maltoni, O. Mattelaer, T. Stelzer, MadGraph5: going beyond, JHEP 1106 (2011) 128, http://dx.doi.org/10.1007/JHEP06(2011)128, arXiv:1106.0522.
[43] S. Frixione, P. Nason, C. Oleari, Matching NLO QCD computations with parton shower simulations: the POWHEG method, JHEP 0711 (2007) 070, http://dx.doi.org/10.1088/1126-6708/2007/11/070, arXiv:0709.2092.
[44] T. Sjöstrand, S. Mrenna, P. Skands, PYTHIA 6.4 physics and manual, JHEP 0605 (2006) 026, http://dx.doi.org/10.1088/1126-6708/2006/05/026, arXiv:hep-ph/0603175.
[45] S. Agostinelli, et al., GEANT4 — a simulation toolkit, Nucl. Instrum. Methods A 506 (2003) 250, http://dx.doi.org/10.1016/S0168-9002(03)01368-8.
[46] N. Kidonakis, Next-to-next-to-leading-order collinear and soft gluon corrections for t-channel single top quark production, Phys. Rev. D 83 (2011) 091503, http://dx.doi.org/10.1103/PhysRevD.83.091503, arXiv:1103.2792.
[47] N. Kidonakis, Differential and total cross sections for top pair and single top production, arXiv:1205.3453, 2012.
[48] R. Gavin, Y. Li, F. Petriello, S. Quackenbush, FEWZ 2.0: A code for hadronic Z production at next-to-next-to-leading order, Comput. Phys. Comm. 182 (2011) 2388, http://dx.doi.org/10.1016/j.cpc.2011.06.008, arXiv:1011.3540.
[49] J.M. Campbell, R.K. Ellis, C. Williams, Vector boson pair production at the LHC, JHEP 1107 (2011) 018, http://dx.doi.org/10.1007/JHEP07(2011)018, arXiv:1105.0020.
[50] CMS Collaboration, Fast simulation of the CMS detector, J. Phys. Conf. Ser. 219 (2010) 032053, http://dx.doi.org/10.1088/1742-6596/219/3/032053, D. Orbaker for the collaboration.
[51] CMS Collaboration, Comparison of the fast simulation of CMS with the first LHC data, CMS Detector Performance Summary CMS-DP-2010-039, http://cdsweb.cern.ch/record/1309890, 2010.
[52] J. Pumplin, D.R. Stump, J. Huston, H.-L. Lai, P. Nadolsky, W.-K. Tung, New generation of parton distributions with uncertainties from global QCD analysis, JHEP 0207 (2002) 012, http://dx.doi.org/10.1088/1126-6708/2002/07/012, arXiv:hep-ph/0201195.
[53] P.M. Nadolsky, H.-L. Lai, Q.-H. Cao, J. Huston, J. Pumplin, D. Stump, W.-K. Tung, C.-P. Yuan, Implications of CTEQ global analysis for collider observables, Phys. Rev. D 78 (2008) 013004, http://dx.doi.org/10.1103/PhysRevD.78.013004, arXiv:0802.0007.
[54] S. Frixione, B.R. Webber, Matching NLO QCD computations and parton shower simulations, JHEP 0206 (2002) 029, http://dx.doi.org/10.1088/1126-6708/2002/06/029, arXiv:hep-ph/0204244.
[55] ATLAS Collaboration, Measurement of the cross section for the production of a W boson in association with b jets in pp collisions at $\sqrt{s} = 7$ TeV with the ATLAS detector, Phys. Lett. B 707 (2012) 418, http://dx.doi.org/10.1016/j.physletb.2011.12.046, arXiv:1109.1470.
[56] CMS Collaboration, Evidence for associated production of a single top quark and W boson in pp collisions at 7 TeV, Phys. Rev. Lett. 110 (2013) 022003, http://dx.doi.org/10.1103/PhysRevLett.110.022003, arXiv:1209.3489.
[57] Particle Data Group, J. Beringer, et al., Review of Particle Physics, Phys. Rev. D 86 (2012) 010001, http://dx.doi.org/10.1103/PhysRevD.86.010001.
[58] CMS Collaboration, CMS luminosity based on pixel cluster counting – summer 2012 update, CMS Physics Analysis Summary CMS-PAS-LUM-12–001, http://cds.cern.ch/record/1482193, 2012.
[59] A.D. Martin, W.J. Stirling, R.S. Thorne, G. Watt, Parton distributions for the LHC, Eur. Phys. J. C 63 (2009) 189, http://dx.doi.org/10.1140/epjc/s10052-009-1072-5, arXiv:0901.0002.
[60] R.D. Ball, V. Bertone, F. Cerutti, L. Del Debbio, S. Forte, A. Guffanti, J.I. Latorre, J. Rojo, M. Ubiali, Impact of heavy quark masses on parton distributions and LHC phenomenology, Nucl. Phys. B 849 (2011) 296, http://dx.doi.org/10.1016/j.nuclphysb.2011.03.021, arXiv:1101.1300.
[61] M. Botje, J. Butterworth, A. Cooper-Sarkar, A. de Roeck, J. Feltesse, S. Forte, A. Glazov, J. Huston, R. McNulty, T. Sjöstrand, The PDF4LHC working group interim recommendations, arXiv:1101.0538, 2011.
[62] M. Krämer, A. Kulesza, R. van der Leeuw, M. Mangano, S. Padhi, T. Plehn, X. Portell, Supersymmetry production cross sections in pp collisions at $\sqrt{s} = 7$ TeV, arXiv:1206.2892, 2012.
[63] T. Junk, Confidence level computation for combining searches with small statistics, Nucl. Instrum. Methods A 434 (1999) 435, http://dx.doi.org/10.1016/S0168-9002(99)00498-2, arXiv:hep-ex/9902006.
[64] A.L. Read, Presentation of search results: the CL_s technique, J. Phys. G 28 (2002) 2693, http://dx.doi.org/10.1088/0954-3899/28/10/313.

CMS Collaboration

S. Chatrchyan, V. Khachatryan, A.M. Sirunyan, A. Tumasyan

Yerevan Physics Institute, Yerevan, Armenia

W. Adam, T. Bergauer, M. Dragicevic, J. Erö, C. Fabjan [1], M. Friedl, R. Frühwirth [1], V.M. Ghete, N. Hörmann, J. Hrubec, M. Jeitler [1], W. Kiesenhofer, V. Knünz, M. Krammer [1], I. Krätschmer, D. Liko, I. Mikulec, D. Rabady [2], B. Rahbaran, C. Rohringer, H. Rohringer, R. Schöfbeck, J. Strauss, A. Taurok, W. Treberer-Treberspurg, W. Waltenberger, C.-E. Wulz [1]

Institut für Hochenergiephysik der OeAW, Wien, Austria

V. Mossolov, N. Shumeiko, J. Suarez Gonzalez

National Centre for Particle and High Energy Physics, Minsk, Belarus

S. Alderweireldt, M. Bansal, S. Bansal, T. Cornelis, E.A. De Wolf, X. Janssen, A. Knutsson, S. Luyckx, L. Mucibello, S. Ochesanu, B. Roland, R. Rougny, Z. Staykova, H. Van Haevermaet, P. Van Mechelen, N. Van Remortel, A. Van Spilbeeck

Universiteit Antwerpen, Antwerpen, Belgium

F. Blekman, S. Blyweert, J. D'Hondt, A. Kalogeropoulos, J. Keaveney, M. Maes, A. Olbrechts, S. Tavernier, W. Van Doninck, P. Van Mulders, G.P. Van Onsem, I. Villella

Vrije Universiteit Brussel, Brussel, Belgium

B. Clerbaux, G. De Lentdecker, L. Favart, A.P.R. Gay, T. Hreus, A. Léonard, P.E. Marage, A. Mohammadi, L. Perniè, T. Reis, T. Seva, L. Thomas, C. Vander Velde, P. Vanlaer, J. Wang

Université Libre de Bruxelles, Bruxelles, Belgium

V. Adler, K. Beernaert, L. Benucci, A. Cimmino, S. Costantini, S. Dildick, G. Garcia, B. Klein, J. Lellouch, A. Marinov, J. Mccartin, A.A. Ocampo Rios, D. Ryckbosch, M. Sigamani, N. Strobbe, F. Thyssen, M. Tytgat, S. Walsh, E. Yazgan, N. Zaganidis

Ghent University, Ghent, Belgium

S. Basegmez, C. Beluffi [3], G. Bruno, R. Castello, A. Caudron, L. Ceard, C. Delaere, T. du Pree, D. Favart, L. Forthomme, A. Giammanco [4], J. Hollar, P. Jez, V. Lemaitre, J. Liao, O. Militaru, C. Nuttens, D. Pagano, A. Pin, K. Piotrzkowski, A. Popov [5], M. Selvaggi, J.M. Vizan Garcia

Université Catholique de Louvain, Louvain-la-Neuve, Belgium

N. Beliy, T. Caebergs, E. Daubie, G.H. Hammad

Université de Mons, Mons, Belgium

G.A. Alves, M. Correa Martins Junior, T. Martins, M.E. Pol, M.H.G. Souza

Centro Brasileiro de Pesquisas Fisicas, Rio de Janeiro, Brazil

W.L. Aldá Júnior, W. Carvalho, J. Chinellato [6], A. Custódio, E.M. Da Costa, D. De Jesus Damiao, C. De Oliveira Martins, S. Fonseca De Souza, H. Malbouisson, M. Malek, D. Matos Figueiredo, L. Mundim, H. Nogima, W.L. Prado Da Silva, A. Santoro, A. Sznajder, E.J. Tonelli Manganote [6], A. Vilela Pereira

Universidade do Estado do Rio de Janeiro, Rio de Janeiro, Brazil

C.A. Bernardes [b], F.A. Dias [a,7], T.R. Fernandez Perez Tomei [a], E.M. Gregores [b], C. Lagana [a], P.G. Mercadante [b], S.F. Novaes [a], Sandra S. Padula [a]

[a] *Universidade Estadual Paulista, São Paulo, Brazil*
[b] *Universidade Federal do ABC, São Paulo, Brazil*

V. Genchev [2], P. Iaydjiev [2], S. Piperov, M. Rodozov, G. Sultanov, M. Vutova

Institute for Nuclear Research and Nuclear Energy, Sofia, Bulgaria

A. Dimitrov, R. Hadjiiska, V. Kozhuharov, L. Litov, B. Pavlov, P. Petkov

University of Sofia, Sofia, Bulgaria

J.G. Bian, G.M. Chen, H.S. Chen, C.H. Jiang, D. Liang, S. Liang, X. Meng, J. Tao, J. Wang,

X. Wang, Z. Wang, H. Xiao, M. Xu

Institute of High Energy Physics, Beijing, China

C. Asawatangtrakuldee, Y. Ban, Y. Guo, Q. Li, W. Li, S. Liu, Y. Mao, S.J. Qian, D. Wang, L. Zhang, W. Zou

State Key Laboratory of Nuclear Physics and Technology, Peking University, Beijing, China

C. Avila, C.A. Carrillo Montoya, L.F. Chaparro Sierra, J.P. Gomez, B. Gomez Moreno, J.C. Sanabria

Universidad de Los Andes, Bogota, Colombia

N. Godinovic, D. Lelas, R. Plestina [8], D. Polic, I. Puljak

Technical University of Split, Split, Croatia

Z. Antunovic, M. Kovac

University of Split, Split, Croatia

V. Brigljevic, S. Duric, K. Kadija, J. Luetic, D. Mekterovic, S. Morovic, L. Tikvica

Institute Rudjer Boskovic, Zagreb, Croatia

A. Attikis, G. Mavromanolakis, J. Mousa, C. Nicolaou, F. Ptochos, P.A. Razis

University of Cyprus, Nicosia, Cyprus

M. Finger, M. Finger Jr.

Charles University, Prague, Czech Republic

Y. Assran [9], S. Elgammal [10], A. Ellithi Kamel [11], M.A. Mahmoud [12], A. Mahrous [13], A. Radi [14,15]

Academy of Scientific Research and Technology of the Arab Republic of Egypt, Egyptian Network of High Energy Physics, Cairo, Egypt

M. Kadastik, M. Müntel, M. Murumaa, M. Raidal, L. Rebane, A. Tiko

National Institute of Chemical Physics and Biophysics, Tallinn, Estonia

P. Eerola, G. Fedi, M. Voutilainen

Department of Physics, University of Helsinki, Helsinki, Finland

J. Härkönen, V. Karimäki, R. Kinnunen, M.J. Kortelainen, T. Lampén, K. Lassila-Perini, S. Lehti, T. Lindén, P. Luukka, T. Mäenpää, T. Peltola, E. Tuominen, J. Tuominiemi, E. Tuovinen, L. Wendland

Helsinki Institute of Physics, Helsinki, Finland

T. Tuuva

Lappeenranta University of Technology, Lappeenranta, Finland

M. Besancon, S. Choudhury, F. Couderc, M. Dejardin, D. Denegri, B. Fabbro, J.L. Faure, F. Ferri, S. Ganjour, A. Givernaud, P. Gras, G. Hamel de Monchenault, P. Jarry, E. Locci, J. Malcles, L. Millischer, A. Nayak, J. Rander, A. Rosowsky, M. Titov

DSM/IRFU, CEA/Saclay, Gif-sur-Yvette, France

S. Baffioni, F. Beaudette, L. Benhabib, M. Bluj [16], P. Busson, C. Charlot, N. Daci, T. Dahms, M. Dalchenko, L. Dobrzynski, A. Florent, R. Granier de Cassagnac, M. Haguenauer, P. Miné,

C. Mironov, I.N. Naranjo, M. Nguyen, C. Ochando, P. Paganini, D. Sabes, R. Salerno, Y. Sirois, C. Veelken, A. Zabi

Laboratoire Leprince-Ringuet, Ecole Polytechnique, IN2P3-CNRS, Palaiseau, France

J.-L. Agram [17], J. Andrea, D. Bloch, D. Bodin, J.-M. Brom, E.C. Chabert, C. Collard, E. Conte [17], F. Drouhin [17], J.-C. Fontaine [17], D. Gelé, U. Goerlach, C. Goetzmann, P. Juillot, A.-C. Le Bihan, P. Van Hove

Institut Pluridisciplinaire Hubert Curien, Université de Strasbourg, Université de Haute Alsace Mulhouse, CNRS/IN2P3, Strasbourg, France

S. Gadrat

Centre de Calcul de l'Institut National de Physique Nucleaire et de Physique des Particules, CNRS/IN2P3, Villeurbanne, France

S. Beauceron, N. Beaupere, G. Boudoul, S. Brochet, J. Chasserat, R. Chierici, D. Contardo, P. Depasse, H. El Mamouni, J. Fay, S. Gascon, M. Gouzevitch, B. Ille, T. Kurca, M. Lethuillier, L. Mirabito, S. Perries, L. Sgandurra, V. Sordini, Y. Tschudi, M. Vander Donckt, P. Verdier, S. Viret

Université de Lyon, Université Claude Bernard Lyon 1, CNRS-IN2P3, Institut de Physique Nucléaire de Lyon, Villeurbanne, France

Z. Tsamalaidze [18]

Institute of High Energy Physics and Informatization, Tbilisi State University, Tbilisi, Georgia

C. Autermann, S. Beranek, B. Calpas, M. Edelhoff, L. Feld, N. Heracleous, O. Hindrichs, K. Klein, A. Ostapchuk, A. Perieanu, F. Raupach, J. Sammet, S. Schael, D. Sprenger, H. Weber, B. Wittmer, V. Zhukov [5]

RWTH Aachen University, I. Physikalisches Institut, Aachen, Germany

M. Ata, J. Caudron, E. Dietz-Laursonn, D. Duchardt, M. Erdmann, R. Fischer, A. Güth, T. Hebbeker, C. Heidemann, K. Hoepfner, D. Klingebiel, P. Kreuzer, M. Merschmeyer, A. Meyer, M. Olschewski, K. Padeken, P. Papacz, H. Pieta, H. Reithler, S.A. Schmitz, L. Sonnenschein, J. Steggemann, D. Teyssier, S. Thüer, M. Weber

RWTH Aachen University, III. Physikalisches Institut A, Aachen, Germany

V. Cherepanov, Y. Erdogan, G. Flügge, H. Geenen, M. Geisler, W. Haj Ahmad, F. Hoehle, B. Kargoll, T. Kress, Y. Kuessel, J. Lingemann [2], A. Nowack, I.M. Nugent, L. Perchalla, O. Pooth, A. Stahl

RWTH Aachen University, III. Physikalisches Institut B, Aachen, Germany

M. Aldaya Martin, I. Asin, N. Bartosik, J. Behr, W. Behrenhoff, U. Behrens, M. Bergholz [19], A. Bethani, K. Borras, A. Burgmeier, A. Cakir, L. Calligaris, A. Campbell, F. Costanza, C. Diez Pardos, S. Dooling, T. Dorland, G. Eckerlin, D. Eckstein, G. Flucke, A. Geiser, I. Glushkov, P. Gunnellini, S. Habib, J. Hauk, G. Hellwig, D. Horton, H. Jung, M. Kasemann, P. Katsas, C. Kleinwort, H. Kluge, M. Krämer, D. Krücker, E. Kuznetsova, W. Lange, J. Leonard, K. Lipka, W. Lohmann [19], B. Lutz, R. Mankel, I. Marfin, I.-A. Melzer-Pellmann, A.B. Meyer, J. Mnich, A. Mussgiller, S. Naumann-Emme, O. Novgorodova, F. Nowak, J. Olzem, H. Perrey, A. Petrukhin, D. Pitzl, R. Placakyte, A. Raspereza, P.M. Ribeiro Cipriano, C. Riedl, E. Ron, M.Ö. Sahin, J. Salfeld-Nebgen, R. Schmidt [19], T. Schoerner-Sadenius, N. Sen, M. Stein, R. Walsh, C. Wissing

Deutsches Elektronen-Synchrotron, Hamburg, Germany

V. Blobel, H. Enderle, J. Erfle, U. Gebbert, M. Görner, M. Gosselink, J. Haller, K. Heine, R.S. Höing, G. Kaussen, H. Kirschenmann, R. Klanner, R. Kogler, J. Lange, I. Marchesini, T. Peiffer, N. Pietsch, D. Rathjens, C. Sander, H. Schettler, P. Schleper, E. Schlieckau,

A. Schmidt, M. Schröder, T. Schum, M. Seidel, J. Sibille [20], V. Sola, H. Stadie, G. Steinbrück, J. Thomsen, D. Troendle, L. Vanelderen

University of Hamburg, Hamburg, Germany

C. Barth, C. Baus, J. Berger, C. Böser, E. Butz, T. Chwalek, W. De Boer, A. Descroix, A. Dierlamm, M. Feindt, M. Guthoff [2], F. Hartmann [2], T. Hauth [2], H. Held, K.H. Hoffmann, U. Husemann, I. Katkov [5], J.R. Komaragiri, A. Kornmayer [2], P. Lobelle Pardo, D. Martschei, Th. Müller, M. Niegel, A. Nürnberg, O. Oberst, J. Ott, G. Quast, K. Rabbertz, F. Ratnikov, S. Röcker, F.-P. Schilling, G. Schott, H.J. Simonis, F.M. Stober, R. Ulrich, J. Wagner-Kuhr, S. Wayand, T. Weiler, M. Zeise

Institut für Experimentelle Kernphysik, Karlsruhe, Germany

G. Anagnostou, G. Daskalakis, T. Geralis, S. Kesisoglou, A. Kyriakis, D. Loukas, A. Markou, C. Markou, E. Ntomari

Institute of Nuclear and Particle Physics (INPP), NCSR Demokritos, Aghia Paraskevi, Greece

L. Gouskos, T.J. Mertzimekis, A. Panagiotou, N. Saoulidou, E. Stiliaris

University of Athens, Athens, Greece

X. Aslanoglou, I. Evangelou, G. Flouris, C. Foudas, P. Kokkas, N. Manthos, I. Papadopoulos, E. Paradas

University of Ioánnina, Ioánnina, Greece

G. Bencze, C. Hajdu, P. Hidas, D. Horvath [21], B. Radics, F. Sikler, V. Veszpremi, G. Vesztergombi [22], A.J. Zsigmond

KFKI Research Institute for Particle and Nuclear Physics, Budapest, Hungary

N. Beni, S. Czellar, J. Molnar, J. Palinkas, Z. Szillasi

Institute of Nuclear Research ATOMKI, Debrecen, Hungary

J. Karancsi, P. Raics, Z.L. Trocsanyi, B. Ujvari

University of Debrecen, Debrecen, Hungary

S.B. Beri, V. Bhatnagar, N. Dhingra, R. Gupta, M. Kaur, M.Z. Mehta, M. Mittal, N. Nishu, L.K. Saini, A. Sharma, J.B. Singh

Panjab University, Chandigarh, India

Ashok Kumar, Arun Kumar, S. Ahuja, A. Bhardwaj, B.C. Choudhary, S. Malhotra, M. Naimuddin, K. Ranjan, P. Saxena, V. Sharma, R.K. Shivpuri

University of Delhi, Delhi, India

S. Banerjee, S. Bhattacharya, K. Chatterjee, S. Dutta, B. Gomber, Sa. Jain, Sh. Jain, R. Khurana, A. Modak, S. Mukherjee, D. Roy, S. Sarkar, M. Sharan

Saha Institute of Nuclear Physics, Kolkata, India

A. Abdulsalam, D. Dutta, S. Kailas, V. Kumar, A.K. Mohanty [2], L.M. Pant, P. Shukla, A. Topkar

Bhabha Atomic Research Centre, Mumbai, India

T. Aziz, R.M. Chatterjee, S. Ganguly, S. Ghosh, M. Guchait [23], A. Gurtu [24], G. Kole, S. Kumar, M. Maity [25], G. Majumder, K. Mazumdar, G.B. Mohanty, B. Parida, K. Sudhakar, N. Wickramage [26]

Tata Institute of Fundamental Research – EHEP, Mumbai, India

S. Banerjee, S. Dugad

Tata Institute of Fundamental Research – HECR, Mumbai, India

H. Arfaei, H. Bakhshiansohi, S.M. Etesami [27], A. Fahim [28], H. Hesari, A. Jafari, M. Khakzad, M. Mohammadi Najafabadi, S. Paktinat Mehdiabadi, B. Safarzadeh [29], M. Zeinali

Institute for Research in Fundamental Sciences (IPM), Tehran, Iran

M. Grunewald

University College Dublin, Dublin, Ireland

M. Abbrescia [a,b], L. Barbone [a,b], C. Calabria [a,b], S.S. Chhibra [a,b], A. Colaleo [a], D. Creanza [a,c], N. De Filippis [a,c], M. De Palma [a,b], L. Fiore [a], G. Iaselli [a,c], G. Maggi [a,c], M. Maggi [a], B. Marangelli [a,b], S. My [a,c], S. Nuzzo [a,b], N. Pacifico [a], A. Pompili [a,b], G. Pugliese [a,c], G. Selvaggi [a,b], L. Silvestris [a], G. Singh [a,b], R. Venditti [a,b], P. Verwilligen [a], G. Zito [a]

[a] *INFN Sezione di Bari, Bari, Italy*
[b] *Università di Bari, Bari, Italy*
[c] *Politecnico di Bari, Bari, Italy*

G. Abbiendi [a], A.C. Benvenuti [a], D. Bonacorsi [a,b], S. Braibant-Giacomelli [a,b], L. Brigliadori [a,b], R. Campanini [a,b], P. Capiluppi [a,b], A. Castro [a,b], F.R. Cavallo [a], M. Cuffiani [a,b], G.M. Dallavalle [a], F. Fabbri [a], A. Fanfani [a,b], D. Fasanella [a,b], P. Giacomelli [a], C. Grandi [a], L. Guiducci [a,b], S. Marcellini [a], G. Masetti [a,2], M. Meneghelli [a,b], A. Montanari [a], F.L. Navarria [a,b], F. Odorici [a], A. Perrotta [a], F. Primavera [a,b], A.M. Rossi [a,b], T. Rovelli [a,b], G.P. Siroli [a,b], N. Tosi [a,b], R. Travaglini [a,b]

[a] *INFN Sezione di Bologna, Bologna, Italy*
[b] *Università di Bologna, Bologna, Italy*

S. Albergo [a,b], M. Chiorboli [a,b], S. Costa [a,b], F. Giordano [a,2], R. Potenza [a,b], A. Tricomi [a,b], C. Tuve [a,b]

[a] *INFN Sezione di Catania, Catania, Italy*
[b] *Università di Catania, Catania, Italy*

G. Barbagli [a], V. Ciulli [a,b], C. Civinini [a], R. D'Alessandro [a,b], E. Focardi [a,b], S. Frosali [a,b], E. Gallo [a], S. Gonzi [a,b], V. Gori [a,b], P. Lenzi [a,b], M. Meschini [a], S. Paoletti [a], G. Sguazzoni [a], A. Tropiano [a,b]

[a] *INFN Sezione di Firenze, Firenze, Italy*
[b] *Università di Firenze, Firenze, Italy*

L. Benussi, S. Bianco, F. Fabbri, D. Piccolo

INFN Laboratori Nazionali di Frascati, Frascati, Italy

P. Fabbricatore [a], R. Musenich [a], S. Tosi [a,b]

[a] *INFN Sezione di Genova, Genova, Italy*
[b] *Università di Genova, Genova, Italy*

A. Benaglia [a], F. De Guio [a,b], L. Di Matteo [a,b], M.E. Dinardo [a,b], S. Fiorendi [a,b], S. Gennai [a], A. Ghezzi [a,b], P. Govoni [a,b], M.T. Lucchini [a,b,2], S. Malvezzi [a], R.A. Manzoni [a,b,2],

A. Martelli [a,b,2], D. Menasce [a], L. Moroni [a], M. Paganoni [a,b], D. Pedrini [a], S. Ragazzi [a,b], N. Redaelli [a], T. Tabarelli de Fatis [a,b]

[a] INFN Sezione di Milano-Bicocca, Milano, Italy
[b] Università di Milano-Bicocca, Milano, Italy

S. Buontempo [a], N. Cavallo [a,c], A. De Cosa [a,b], F. Fabozzi [a,c], A.O.M. Iorio [a,b], L. Lista [a], S. Meola [a,d,2], M. Merola [a], P. Paolucci [a,2]

[a] INFN Sezione di Napoli, Napoli, Italy
[b] Università di Napoli 'Federico II', Napoli, Italy
[c] Università della Basilicata (Potenza), Napoli, Italy
[d] Università G. Marconi (Roma), Napoli, Italy

P. Azzi [a], N. Bacchetta [a], D. Bisello [a,b], A. Branca [a,b], R. Carlin [a,b], P. Checchia [a], T. Dorigo [a], U. Dosselli [a], M. Galanti [a,b,2], F. Gasparini [a,b], U. Gasparini [a,b], P. Giubilato [a,b], A. Gozzelino [a], M. Gulmini [a,30], K. Kanishchev [a,c], S. Lacaprara [a], I. Lazzizzera [a,c], M. Margoni [a,b], G. Maron [a,30], A.T. Meneguzzo [a,b], M. Michelotto [a], J. Pazzini [a,b], N. Pozzobon [a,b], P. Ronchese [a,b], F. Simonetto [a,b], E. Torassa [a], M. Tosi [a,b], S. Vanini [a,b], P. Zotto [a,b], G. Zumerle [a,b]

[a] INFN Sezione di Padova, Padova, Italy
[b] Università di Padova, Padova, Italy
[c] Università di Trento (Trento), Padova, Italy

M. Gabusi [a,b], S.P. Ratti [a,b], C. Riccardi [a,b], P. Vitulo [a,b]

[a] INFN Sezione di Pavia, Pavia, Italy
[b] Università di Pavia, Pavia, Italy

M. Biasini [a,b], G.M. Bilei [a], L. Fanò [a,b], P. Lariccia [a,b], G. Mantovani [a,b], M. Menichelli [a], A. Nappi [a,b,†], F. Romeo [a,b], A. Saha [a], A. Santocchia [a,b], A. Spiezia [a,b]

[a] INFN Sezione di Perugia, Perugia, Italy
[b] Università di Perugia, Perugia, Italy

K. Androsov [a,31], P. Azzurri [a], G. Bagliesi [a], J. Bernardini [a], T. Boccali [a], G. Broccolo [a,c], R. Castaldi [a], R.T. D'Agnolo [a,c,2], R. Dell'Orso [a], F. Fiori [a,c], L. Foà [a,c], A. Giassi [a], M.T. Grippo [a,31], A. Kraan [a], F. Ligabue [a,c], T. Lomtadze [a], L. Martini [a,31], A. Messineo [a,b], F. Palla [a], A. Rizzi [a,b], A. Savoy-Navarro [a,32], A.T. Serban [a], P. Spagnolo [a], P. Squillacioti [a], R. Tenchini [a], G. Tonelli [a,b], A. Venturi [a], P.G. Verdini [a], C. Vernieri [a,c]

[a] INFN Sezione di Pisa, Pisa, Italy
[b] Università di Pisa, Pisa, Italy
[c] Scuola Normale Superiore di Pisa, Pisa, Italy

L. Barone [a,b], F. Cavallari [a], D. Del Re [a,b], M. Diemoz [a], M. Grassi [a,b,2], E. Longo [a,b], F. Margaroli [a,b], P. Meridiani [a], F. Micheli [a,b], S. Nourbakhsh [a,b], G. Organtini [a,b], R. Paramatti [a], S. Rahatlou [a,b], L. Soffi [a,b]

[a] INFN Sezione di Roma, Roma, Italy
[b] Università di Roma, Roma, Italy

N. Amapane [a,b], R. Arcidiacono [a,c], S. Argiro [a,b], M. Arneodo [a,c], C. Biino [a], N. Cartiglia [a], S. Casasso [a,b], M. Costa [a,b], N. Demaria [a], C. Mariotti [a], S. Maselli [a], E. Migliore [a,b], V. Monaco [a,b], M. Musich [a], M.M. Obertino [a,c], G. Ortona [a,b], N. Pastrone [a], M. Pelliccioni [a,2], A. Potenza [a,b], A. Romero [a,b], M. Ruspa [a,c], R. Sacchi [a,b], A. Solano [a,b], A. Staiano [a], U. Tamponi [a]

[a] INFN Sezione di Torino, Torino, Italy
[b] Università di Torino, Torino, Italy
[c] Università del Piemonte Orientale (Novara), Torino, Italy

S. Belforte [a], V. Candelise [a,b], M. Casarsa [a], F. Cossutti [a,2], G. Della Ricca [a,b], B. Gobbo [a], C. La Licata [a,b], M. Marone [a,b], D. Montanino [a,b], A. Penzo [a], A. Schizzi [a,b], A. Zanetti [a]

[a] *INFN Sezione di Trieste, Trieste, Italy*
[b] *Università di Trieste, Trieste, Italy*

S. Chang, T.Y. Kim, S.K. Nam

Kangwon National University, Chunchon, Republic of Korea

D.H. Kim, G.N. Kim, J.E. Kim, D.J. Kong, Y.D. Oh, H. Park, D.C. Son

Kyungpook National University, Daegu, Republic of Korea

J.Y. Kim, Zero J. Kim, S. Song

Chonnam National University, Institute for Universe and Elementary Particles, Kwangju, Republic of Korea

S. Choi, D. Gyun, B. Hong, M. Jo, H. Kim, T.J. Kim, K.S. Lee, S.K. Park, Y. Roh

Korea University, Seoul, Republic of Korea

M. Choi, J.H. Kim, C. Park, I.C. Park, S. Park, G. Ryu

University of Seoul, Seoul, Republic of Korea

Y. Choi, Y.K. Choi, J. Goh, M.S. Kim, E. Kwon, B. Lee, J. Lee, S. Lee, H. Seo, I. Yu

Sungkyunkwan University, Suwon, Republic of Korea

I. Grigelionis, A. Juodagalvis

Vilnius University, Vilnius, Lithuania

H. Castilla-Valdez, E. De La Cruz-Burelo, I. Heredia-de La Cruz [33], R. Lopez-Fernandez, J. Martínez-Ortega, A. Sanchez-Hernandez, L.M. Villasenor-Cendejas

Centro de Investigacion y de Estudios Avanzados del IPN, Mexico City, Mexico

S. Carrillo Moreno, F. Vazquez Valencia

Universidad Iberoamericana, Mexico City, Mexico

H.A. Salazar Ibarguen

Benemerita Universidad Autonoma de Puebla, Puebla, Mexico

E. Casimiro Linares, A. Morelos Pineda, M.A. Reyes-Santos

Universidad Autónoma de San Luis Potosí, San Luis Potosí, Mexico

D. Krofcheck

University of Auckland, Auckland, New Zealand

A.J. Bell, P.H. Butler, R. Doesburg, S. Reucroft, H. Silverwood

University of Canterbury, Christchurch, New Zealand

M. Ahmad, M.I. Asghar, J. Butt, H.R. Hoorani, S. Khalid, W.A. Khan, T. Khurshid, S. Qazi, M.A. Shah, M. Shoaib

National Centre for Physics, Quaid-I-Azam University, Islamabad, Pakistan

H. Bialkowska, B. Boimska, T. Frueboes, M. Górski, M. Kazana, K. Nawrocki,

K. Romanowska-Rybinska, M. Szleper, G. Wrochna, P. Zalewski

National Centre for Nuclear Research, Swierk, Poland

G. Brona, K. Bunkowski, M. Cwiok, W. Dominik, K. Doroba, A. Kalinowski, M. Konecki, J. Krolikowski, M. Misiura, W. Wolszczak

Institute of Experimental Physics, Faculty of Physics, University of Warsaw, Warsaw, Poland

N. Almeida, P. Bargassa, C. Beirão Da Cruz E Silva, P. Faccioli, P.G. Ferreira Parracho, M. Gallinaro, J. Rodrigues Antunes, J. Seixas [2], J. Varela, P. Vischia

Laboratório de Instrumentação e Física Experimental de Partículas, Lisboa, Portugal

P. Bunin, M. Gavrilenko, I. Golutvin, I. Gorbunov, A. Kamenev, V. Karjavin, V. Konoplyanikov, G. Kozlov, A. Lanev, A. Malakhov, V. Matveev, P. Moisenz, V. Palichik, V. Perelygin, S. Shmatov, N. Skatchkov, V. Smirnov, A. Zarubin

Joint Institute for Nuclear Research, Dubna, Russia

S. Evstyukhin, V. Golovtsov, Y. Ivanov, V. Kim, P. Levchenko, V. Murzin, V. Oreshkin, I. Smirnov, V. Sulimov, L. Uvarov, S. Vavilov, A. Vorobyev, An. Vorobyev

Petersburg Nuclear Physics Institute, Gatchina (St. Petersburg), Russia

Yu. Andreev, A. Dermenev, S. Gninenko, N. Golubev, M. Kirsanov, N. Krasnikov, A. Pashenkov, D. Tlisov, A. Toropin

Institute for Nuclear Research, Moscow, Russia

V. Epshteyn, M. Erofeeva, V. Gavrilov, N. Lychkovskaya, V. Popov, G. Safronov, S. Semenov, A. Spiridonov, V. Stolin, E. Vlasov, A. Zhokin

Institute for Theoretical and Experimental Physics, Moscow, Russia

V. Andreev, M. Azarkin, I. Dremin, M. Kirakosyan, A. Leonidov, G. Mesyats, S.V. Rusakov, A. Vinogradov

P.N. Lebedev Physical Institute, Moscow, Russia

A. Belyaev, E. Boos, M. Dubinin [7], L. Dudko, A. Ershov, A. Gribushin, V. Klyukhin, O. Kodolova, I. Lokhtin, A. Markina, S. Obraztsov, S. Petrushanko, V. Savrin, A. Snigirev

Skobeltsyn Institute of Nuclear Physics, Lomonosov Moscow State University, Moscow, Russia

I. Azhgirey, I. Bayshev, S. Bitioukov, V. Kachanov, A. Kalinin, D. Konstantinov, V. Krychkine, V. Petrov, R. Ryutin, A. Sobol, L. Tourtchanovitch, S. Troshin, N. Tyurin, A. Uzunian, A. Volkov

State Research Center of Russian Federation, Institute for High Energy Physics, Protvino, Russia

P. Adzic [34], M. Ekmedzic, D. Krpic [34], J. Milosevic

University of Belgrade, Faculty of Physics and Vinca Institute of Nuclear Sciences, Belgrade, Serbia

M. Aguilar-Benitez, J. Alcaraz Maestre, C. Battilana, E. Calvo, M. Cerrada, M. Chamizo Llatas [2], N. Colino, B. De La Cruz, A. Delgado Peris, D. Domínguez Vázquez, C. Fernandez Bedoya, J.P. Fernández Ramos, A. Ferrando, J. Flix, M.C. Fouz, P. Garcia-Abia, O. Gonzalez Lopez, S. Goy Lopez, J.M. Hernandez, M.I. Josa, G. Merino, E. Navarro De Martino, J. Puerta Pelayo, A. Quintario Olmeda, I. Redondo, L. Romero, J. Santaolalla, M.S. Soares, C. Willmott

Centro de Investigaciones Energéticas Medioambientales y Tecnológicas (CIEMAT), Madrid, Spain

C. Albajar, J.F. de Trocóniz

Universidad Autónoma de Madrid, Madrid, Spain

H. Brun, J. Cuevas, J. Fernandez Menendez, S. Folgueras, I. Gonzalez Caballero, L. Lloret Iglesias, J. Piedra Gomez

Universidad de Oviedo, Oviedo, Spain

J.A. Brochero Cifuentes, I.J. Cabrillo, A. Calderon, S.H. Chuang, J. Duarte Campderros, M. Fernandez, G. Gomez, J. Gonzalez Sanchez, A. Graziano, C. Jorda, A. Lopez Virto, J. Marco, R. Marco, C. Martinez Rivero, F. Matorras, F.J. Munoz Sanchez, T. Rodrigo, A.Y. Rodríguez-Marrero, A. Ruiz-Jimeno, L. Scodellaro, I. Vila, R. Vilar Cortabitarte

Instituto de Física de Cantabria (IFCA), CSIC-Universidad de Cantabria, Santander, Spain

D. Abbaneo, E. Auffray, G. Auzinger, M. Bachtis, P. Baillon, A.H. Ball, D. Barney, J. Bendavid, J.F. Benitez, C. Bernet [8], G. Bianchi, P. Bloch, A. Bocci, A. Bonato, O. Bondu, C. Botta, H. Breuker, T. Camporesi, G. Cerminara, T. Christiansen, J.A. Coarasa Perez, S. Colafranceschi [35], D. d'Enterria, A. Dabrowski, A. David, A. De Roeck, S. De Visscher, S. Di Guida, M. Dobson, N. Dupont-Sagorin, A. Elliott-Peisert, J. Eugster, W. Funk, G. Georgiou, M. Giffels, D. Gigi, K. Gill, D. Giordano, M. Girone, M. Giunta, F. Glege, R. Gomez-Reino Garrido, S. Gowdy, R. Guida, J. Hammer, M. Hansen, P. Harris, C. Hartl, A. Hinzmann, V. Innocente, P. Janot, E. Karavakis, K. Kousouris, K. Krajczar, P. Lecoq, Y.-J. Lee, C. Lourenço, N. Magini, M. Malberti, L. Malgeri, M. Mannelli, L. Masetti, F. Meijers, S. Mersi, E. Meschi, R. Moser, M. Mulders, P. Musella, E. Nesvold, L. Orsini, E. Palencia Cortezon, E. Perez, L. Perrozzi, A. Petrilli, A. Pfeiffer, M. Pierini, M. Pimiä, D. Piparo, M. Plagge, L. Quertenmont, A. Racz, W. Reece, G. Rolandi [36], C. Rovelli [37], M. Rovere, H. Sakulin, F. Santanastasio, C. Schäfer, C. Schwick, I. Segoni, S. Sekmen, A. Sharma, P. Siegrist, P. Silva, M. Simon, P. Sphicas [38], D. Spiga, M. Stoye, A. Tsirou, G.I. Veres [22], J.R. Vlimant, H.K. Wöhri, S.D. Worm [39], W.D. Zeuner

CERN, European Organization for Nuclear Research, Geneva, Switzerland

W. Bertl, K. Deiters, W. Erdmann, K. Gabathuler, R. Horisberger, Q. Ingram, H.C. Kaestli, S. König, D. Kotlinski, U. Langenegger, D. Renker, T. Rohe

Paul Scherrer Institut, Villigen, Switzerland

F. Bachmair, L. Bäni, L. Bianchini, P. Bortignon, M.A. Buchmann, B. Casal, N. Chanon, A. Deisher, G. Dissertori, M. Dittmar, M. Donegà, M. Dünser, P. Eller, K. Freudenreich, C. Grab, D. Hits, P. Lecomte, W. Lustermann, A.C. Marini, P. Martinez Ruiz del Arbol, N. Mohr, F. Moortgat, C. Nägeli [40], P. Nef, F. Nessi-Tedaldi, F. Pandolfi, L. Pape, F. Pauss, M. Peruzzi, F.J. Ronga, M. Rossini, L. Sala, A.K. Sanchez, A. Starodumov [41], B. Stieger, M. Takahashi, L. Tauscher [†], A. Thea, K. Theofilatos, D. Treille, C. Urscheler, R. Wallny, H.A. Weber

Institute for Particle Physics, ETH Zurich, Zurich, Switzerland

C. Amsler [42], V. Chiochia, C. Favaro, M. Ivova Rikova, B. Kilminster, B. Millan Mejias, P. Otiougova, P. Robmann, H. Snoek, S. Taroni, S. Tupputi, M. Verzetti

Universität Zürich, Zurich, Switzerland

M. Cardaci, K.H. Chen, C. Ferro, C.M. Kuo, S.W. Li, W. Lin, Y.J. Lu, R. Volpe, S.S. Yu

National Central University, Chung-Li, Taiwan

P. Bartalini, P. Chang, Y.H. Chang, Y.W. Chang, Y. Chao, K.F. Chen, C. Dietz, U. Grundler, W.-S. Hou, Y. Hsiung, K.Y. Kao, Y.J. Lei, R.-S. Lu, D. Majumder, E. Petrakou, X. Shi, J.G. Shiu, Y.M. Tzeng, M. Wang

National Taiwan University (NTU), Taipei, Taiwan

B. Asavapibhop, N. Suwonjandee

Chulalongkorn University, Bangkok, Thailand

A. Adiguzel, M.N. Bakirci [43], S. Cerci [44], C. Dozen, I. Dumanoglu, E. Eskut, S. Girgis, G. Gokbulut, E. Gurpinar, I. Hos, E.E. Kangal, A. Kayis Topaksu, G. Onengut [45], K. Ozdemir, S. Ozturk [43], A. Polatoz, K. Sogut [46], D. Sunar Cerci [44], B. Tali [44], H. Topakli [43], M. Vergili

Cukurova University, Adana, Turkey

I.V. Akin, T. Aliev, B. Bilin, S. Bilmis, M. Deniz, H. Gamsizkan, A.M. Guler, G. Karapinar [47], K. Ocalan, A. Ozpineci, M. Serin, R. Sever, U.E. Surat, M. Yalvac, M. Zeyrek

Middle East Technical University, Physics Department, Ankara, Turkey

E. Gülmez, B. Isildak [48], M. Kaya [49], O. Kaya [49], S. Ozkorucuklu [50], N. Sonmez [51]

Bogazici University, Istanbul, Turkey

H. Bahtiyar [52], E. Barlas, K. Cankocak, Y.O. Günaydin [53], F.I. Vardarlı, M. Yücel

Istanbul Technical University, Istanbul, Turkey

L. Levchuk, P. Sorokin

National Scientific Center, Kharkov Institute of Physics and Technology, Kharkov, Ukraine

J.J. Brooke, E. Clement, D. Cussans, H. Flacher, R. Frazier, J. Goldstein, M. Grimes, G.P. Heath, H.F. Heath, L. Kreczko, S. Metson, D.M. Newbold [39], K. Nirunpong, A. Poll, S. Senkin, V.J. Smith, T. Williams

University of Bristol, Bristol, United Kingdom

L. Basso [54], K.W. Bell, A. Belyaev [54], C. Brew, R.M. Brown, D.J.A. Cockerill, J.A. Coughlan, K. Harder, S. Harper, J. Jackson, E. Olaiya, D. Petyt, B.C. Radburn-Smith, C.H. Shepherd-Themistocleous, I.R. Tomalin, W.J. Womersley

Rutherford Appleton Laboratory, Didcot, United Kingdom

R. Bainbridge, O. Buchmuller, D. Burton, D. Colling, N. Cripps, M. Cutajar, P. Dauncey, G. Davies, M. Della Negra, W. Ferguson, J. Fulcher, D. Futyan, A. Gilbert, A. Guneratne Bryer, G. Hall, Z. Hatherell, J. Hays, G. Iles, M. Jarvis, G. Karapostoli, M. Kenzie, R. Lane, R. Lucas [39], L. Lyons, A.-M. Magnan, J. Marrouche, B. Mathias, R. Nandi, J. Nash, A. Nikitenko [41], J. Pela, M. Pesaresi, K. Petridis, M. Pioppi [55], D.M. Raymond, S. Rogerson, A. Rose, C. Seez, P. Sharp [†], A. Sparrow, A. Tapper, M. Vazquez Acosta, T. Virdee, S. Wakefield, N. Wardle, T. Whyntie

Imperial College, London, United Kingdom

M. Chadwick, J.E. Cole, P.R. Hobson, A. Khan, P. Kyberd, D. Leggat, D. Leslie, W. Martin, I.D. Reid, P. Symonds, L. Teodorescu, M. Turner

Brunel University, Uxbridge, United Kingdom

J. Dittmann, K. Hatakeyama, A. Kasmi, H. Liu, T. Scarborough

Baylor University, Waco, USA

O. Charaf, S.I. Cooper, C. Henderson, P. Rumerio

The University of Alabama, Tuscaloosa, USA

A. Avetisyan, T. Bose, C. Fantasia, A. Heister, P. Lawson, D. Lazic, J. Rohlf, D. Sperka, J. St. John, L. Sulak

Boston University, Boston, USA

J. Alimena, S. Bhattacharya, G. Christopher, D. Cutts, Z. Demiragli, A. Ferapontov, A. Garabedian, U. Heintz, G. Kukartsev, E. Laird, G. Landsberg, M. Luk, M. Narain, M. Segala, T. Sinthuprasith, T. Speer

Brown University, Providence, USA

R. Breedon, G. Breto, M. Calderon De La Barca Sanchez, S. Chauhan, M. Chertok, J. Conway, R. Conway, P.T. Cox, R. Erbacher, M. Gardner, R. Houtz, W. Ko, A. Kopecky, R. Lander, O. Mall, T. Miceli, R. Nelson, D. Pellett, F. Ricci-Tam, B. Rutherford, M. Searle, J. Smith, M. Squires, M. Tripathi, S. Wilbur, R. Yohay

University of California, Davis, Davis, USA

V. Andreev, D. Cline, R. Cousins, S. Erhan, P. Everaerts, C. Farrell, M. Felcini, J. Hauser, M. Ignatenko, C. Jarvis, G. Rakness, P. Schlein †, E. Takasugi, P. Traczyk, V. Valuev, M. Weber

University of California, Los Angeles, USA

J. Babb, R. Clare, J. Ellison, J.W. Gary, G. Hanson, P. Jandir, H. Liu, O.R. Long, A. Luthra, H. Nguyen, S. Paramesvaran, J. Sturdy, S. Sumowidagdo, R. Wilken, S. Wimpenny

University of California, Riverside, Riverside, USA

W. Andrews, J.G. Branson, G.B. Cerati, S. Cittolin, D. Evans, A. Holzner, R. Kelley, M. Lebourgeois, J. Letts, I. Macneill, B. Mangano, S. Padhi, C. Palmer, G. Petrucciani, M. Pieri, M. Sani, V. Sharma, S. Simon, E. Sudano, M. Tadel, Y. Tu, A. Vartak, S. Wasserbaech [56], F. Würthwein, A. Yagil, J. Yoo

University of California, San Diego, La Jolla, USA

D. Barge, R. Bellan, C. Campagnari, M. D'Alfonso, T. Danielson, K. Flowers, P. Geffert, C. George, F. Golf, J. Incandela, C. Justus, P. Kalavase, D. Kovalskyi, V. Krutelyov, S. Lowette, R. Magaña Villalba, N. Mccoll, V. Pavlunin, J. Ribnik, J. Richman, R. Rossin, D. Stuart, W. To, C. West

University of California, Santa Barbara, Santa Barbara, USA

A. Apresyan, A. Bornheim, J. Bunn, Y. Chen, E. Di Marco, J. Duarte, D. Kcira, Y. Ma, A. Mott, H.B. Newman, C. Rogan, M. Spiropulu, V. Timciuc, J. Veverka, R. Wilkinson, S. Xie, Y. Yang, R.Y. Zhu

California Institute of Technology, Pasadena, USA

V. Azzolini, A. Calamba, R. Carroll, T. Ferguson, Y. Iiyama, D.W. Jang, Y.F. Liu, M. Paulini, J. Russ, H. Vogel, I. Vorobiev

Carnegie Mellon University, Pittsburgh, USA

J.P. Cumalat, B.R. Drell, W.T. Ford, A. Gaz, E. Luiggi Lopez, T. Mulholland, U. Nauenberg, J.G. Smith, K. Stenson, K.A. Ulmer, S.R. Wagner

University of Colorado at Boulder, Boulder, USA

J. Alexander, A. Chatterjee, N. Eggert, L.K. Gibbons, W. Hopkins, A. Khukhunaishvili, B. Kreis, N. Mirman, G. Nicolas Kaufman, J.R. Patterson, A. Ryd, E. Salvati, W. Sun, W.D. Teo, J. Thom, J. Thompson, J. Tucker, Y. Weng, L. Winstrom, P. Wittich

Cornell University, Ithaca, USA

D. Winn

Fairfield University, Fairfield, USA

S. Abdullin, M. Albrow, J. Anderson, G. Apollinari, L.A.T. Bauerdick, A. Beretvas, J. Berryhill, P.C. Bhat, K. Burkett, J.N. Butler, V. Chetluru, H.W.K. Cheung, F. Chlebana, S. Cihangir, V.D. Elvira, I. Fisk, J. Freeman, Y. Gao, E. Gottschalk, L. Gray, D. Green, O. Gutsche, D. Hare, R.M. Harris, J. Hirschauer, B. Hooberman, S. Jindariani, M. Johnson, U. Joshi, B. Klima, S. Kunori, S. Kwan, J. Linacre, D. Lincoln, R. Lipton, J. Lykken, K. Maeshima, J.M. Marraffino, V.I. Martinez Outschoorn, S. Maruyama, D. Mason, P. McBride, K. Mishra, S. Mrenna, Y. Musienko [57], C. Newman-Holmes, V. O'Dell, O. Prokofyev, N. Ratnikova, E. Sexton-Kennedy, S. Sharma, W.J. Spalding, L. Spiegel, L. Taylor, S. Tkaczyk, N.V. Tran, L. Uplegger, E.W. Vaandering, R. Vidal, J. Whitmore, W. Wu, F. Yang, J.C. Yun

Fermi National Accelerator Laboratory, Batavia, USA

D. Acosta, P. Avery, D. Bourilkov, M. Chen, T. Cheng, S. Das, M. De Gruttola, G.P. Di Giovanni, D. Dobur, A. Drozdetskiy, R.D. Field, M. Fisher, Y. Fu, I.K. Furic, J. Hugon, B. Kim, J. Konigsberg, A. Korytov, A. Kropivnitskaya, T. Kypreos, J.F. Low, K. Matchev, P. Milenovic [58], G. Mitselmakher, L. Muniz, R. Remington, A. Rinkevicius, N. Skhirtladze, M. Snowball, J. Yelton, M. Zakaria

University of Florida, Gainesville, USA

V. Gaultney, S. Hewamanage, L.M. Lebolo, S. Linn, P. Markowitz, G. Martinez, J.L. Rodriguez

Florida International University, Miami, USA

T. Adams, A. Askew, J. Bochenek, J. Chen, B. Diamond, S.V. Gleyzer, J. Haas, S. Hagopian, V. Hagopian, K.F. Johnson, H. Prosper, V. Veeraraghavan, M. Weinberg

Florida State University, Tallahassee, USA

M.M. Baarmand, B. Dorney, M. Hohlmann, H. Kalakhety, F. Yumiceva

Florida Institute of Technology, Melbourne, USA

M.R. Adams, L. Apanasevich, V.E. Bazterra, R.R. Betts, I. Bucinskaite, J. Callner, R. Cavanaugh, O. Evdokimov, L. Gauthier, C.E. Gerber, D.J. Hofman, S. Khalatyan, P. Kurt, F. Lacroix, D.H. Moon, C. O'Brien, C. Silkworth, D. Strom, P. Turner, N. Varelas

University of Illinois at Chicago (UIC), Chicago, USA

U. Akgun, E.A. Albayrak [52], B. Bilki [59], W. Clarida, K. Dilsiz, F. Duru, S. Griffiths, J.-P. Merlo, H. Mermerkaya [60], A. Mestvirishvili, A. Moeller, J. Nachtman, C.R. Newsom, H. Ogul, Y. Onel, F. Ozok [52], S. Sen, P. Tan, E. Tiras, J. Wetzel, T. Yetkin [61], K. Yi

The University of Iowa, Iowa City, USA

B.A. Barnett, B. Blumenfeld, S. Bolognesi, D. Fehling, G. Giurgiu, A.V. Gritsan, G. Hu, P. Maksimovic, M. Swartz, A. Whitbeck

Johns Hopkins University, Baltimore, USA

P. Baringer, A. Bean, G. Benelli, R.P. Kenny III, M. Murray, D. Noonan, S. Sanders,

R. Stringer, J.S. Wood

The University of Kansas, Lawrence, USA

A.F. Barfuss, I. Chakaberia, A. Ivanov, S. Khalil, M. Makouski, Y. Maravin, S. Shrestha, I. Svintradze

Kansas State University, Manhattan, USA

J. Gronberg, D. Lange, F. Rebassoo, D. Wright

Lawrence Livermore National Laboratory, Livermore, USA

A. Baden, B. Calvert, S.C. Eno, J.A. Gomez, N.J. Hadley, R.G. Kellogg, T. Kolberg, Y. Lu, M. Marionneau, A.C. Mignerey, K. Pedro, A. Peterman, A. Skuja, J. Temple, M.B. Tonjes, S.C. Tonwar

University of Maryland, College Park, USA

A. Apyan, G. Bauer, W. Busza, I.A. Cali, M. Chan, V. Dutta, G. Gomez Ceballos, M. Goncharov, Y. Kim, M. Klute, Y.S. Lai, A. Levin, P.D. Luckey, T. Ma, S. Nahn, C. Paus, D. Ralph, C. Roland, G. Roland, G.S.F. Stephans, F. Stöckli, K. Sumorok, D. Velicanu, R. Wolf, B. Wyslouch, M. Yang, Y. Yilmaz, A.S. Yoon, M. Zanetti, V. Zhukova

Massachusetts Institute of Technology, Cambridge, USA

B. Dahmes, A. De Benedetti, G. Franzoni, A. Gude, J. Haupt, S.C. Kao, K. Klapoetke, Y. Kubota, J. Mans, N. Pastika, R. Rusack, M. Sasseville, A. Singovsky, N. Tambe, J. Turkewitz

University of Minnesota, Minneapolis, USA

L.M. Cremaldi, R. Kroeger, L. Perera, R. Rahmat, D.A. Sanders, D. Summers

University of Mississippi, Oxford, USA

E. Avdeeva, K. Bloom, S. Bose, D.R. Claes, A. Dominguez, M. Eads, R. Gonzalez Suarez, J. Keller, I. Kravchenko, J. Lazo-Flores, S. Malik, F. Meier, G.R. Snow

University of Nebraska-Lincoln, Lincoln, USA

J. Dolen, A. Godshalk, I. Iashvili, S. Jain, A. Kharchilava, A. Kumar, S. Rappoccio, Z. Wan

State University of New York at Buffalo, Buffalo, USA

G. Alverson [*], E. Barberis, D. Baumgartel, M. Chasco, J. Haley, A. Massironi, D. Nash, T. Orimoto, D. Trocino, D. Wood, J. Zhang

Northeastern University, Boston, USA

A. Anastassov, K.A. Hahn, A. Kubik, L. Lusito, N. Mucia, N. Odell, B. Pollack, A. Pozdnyakov, M. Schmitt, S. Stoynev, K. Sung, M. Velasco, S. Won

Northwestern University, Evanston, USA

D. Berry, A. Brinkerhoff, K.M. Chan, M. Hildreth, C. Jessop, D.J. Karmgard, J. Kolb, K. Lannon, W. Luo, S. Lynch, N. Marinelli, D.M. Morse, T. Pearson, M. Planer, R. Ruchti, J. Slaunwhite, N. Valls, M. Wayne, M. Wolf

University of Notre Dame, Notre Dame, USA

L. Antonelli, B. Bylsma, L.S. Durkin, C. Hill, R. Hughes, K. Kotov, T.Y. Ling, D. Puigh, M. Rodenburg, G. Smith, C. Vuosalo, G. Williams, B.L. Winer, H. Wolfe

The Ohio State University, Columbus, USA

E. Berry, P. Elmer, V. Halyo, P. Hebda, J. Hegeman, A. Hunt, P. Jindal, S.A. Koay, D. Lopes Pegna, P. Lujan, D. Marlow, T. Medvedeva, M. Mooney, J. Olsen, P. Piroué, X. Quan, A. Raval, H. Saka, D. Stickland, C. Tully, J.S. Werner, S.C. Zenz, A. Zuranski

Princeton University, Princeton, USA

E. Brownson, A. Lopez, H. Mendez, J.E. Ramirez Vargas

University of Puerto Rico, Mayaguez, USA

E. Alagoz, D. Benedetti, G. Bolla, D. Bortoletto, M. De Mattia, A. Everett, Z. Hu, M. Jones, K. Jung, O. Koybasi, M. Kress, N. Leonardo, V. Maroussov, P. Merkel, D.H. Miller, N. Neumeister, I. Shipsey, D. Silvers, A. Svyatkovskiy, M. Vidal Marono, F. Wang, L. Xu, H.D. Yoo, J. Zablocki, Y. Zheng

Purdue University, West Lafayette, USA

S. Guragain, N. Parashar

Purdue University Calumet, Hammond, USA

A. Adair, B. Akgun, K.M. Ecklund, F.J.M. Geurts, W. Li, B.P. Padley, R. Redjimi, J. Roberts, J. Zabel

Rice University, Houston, USA

B. Betchart, A. Bodek, R. Covarelli, P. de Barbaro, R. Demina, Y. Eshaq, T. Ferbel, A. Garcia-Bellido, P. Goldenzweig, J. Han, A. Harel, D.C. Miner, G. Petrillo, D. Vishnevskiy, M. Zielinski

University of Rochester, Rochester, USA

A. Bhatti, R. Ciesielski, L. Demortier, K. Goulianos, G. Lungu, S. Malik, C. Mesropian

The Rockefeller University, New York, USA

S. Arora, A. Barker, J.P. Chou, C. Contreras-Campana, E. Contreras-Campana, D. Duggan, D. Ferencek, Y. Gershtein, R. Gray, E. Halkiadakis, D. Hidas, A. Lath, S. Panwalkar, M. Park, R. Patel, V. Rekovic, J. Robles, S. Salur, S. Schnetzer, C. Seitz, S. Somalwar, R. Stone, S. Thomas, M. Walker

Rutgers, The State University of New Jersey, Piscataway, USA

G. Cerizza, M. Hollingsworth, K. Rose, S. Spanier, Z.C. Yang, A. York

University of Tennessee, Knoxville, USA

R. Eusebi, W. Flanagan, J. Gilmore, T. Kamon [62], V. Khotilovich, R. Montalvo, I. Osipenkov, Y. Pakhotin, A. Perloff, J. Roe, A. Safonov, T. Sakuma, I. Suarez, A. Tatarinov, D. Toback

Texas A&M University, College Station, USA

N. Akchurin, J. Damgov, C. Dragoiu, P.R. Dudero, C. Jeong, K. Kovitanggoon, S.W. Lee, T. Libeiro, I. Volobouev

Texas Tech University, Lubbock, USA

E. Appelt, A.G. Delannoy, S. Greene, A. Gurrola, W. Johns, C. Maguire, Y. Mao, A. Melo, M. Sharma, P. Sheldon, B. Snook, S. Tuo, J. Velkovska

Vanderbilt University, Nashville, USA

M.W. Arenton, S. Boutle, B. Cox, B. Francis, J. Goodell, R. Hirosky, A. Ledovskoy, C. Lin, C. Neu, J. Wood

University of Virginia, Charlottesville, USA

S. Gollapinni, R. Harr, P.E. Karchin, C. Kottachchi Kankanamge Don, P. Lamichhane, A. Sakharov

Wayne State University, Detroit, USA

D.A. Belknap, L. Borrello, D. Carlsmith, M. Cepeda, S. Dasu, E. Friis, M. Grothe, R. Hall-Wilton, M. Herndon, A. Hervé, K. Kaadze, P. Klabbers, J. Klukas, A. Lanaro, R. Loveless, A. Mohapatra, M.U. Mozer, I. Ojalvo, G.A. Pierro, G. Polese, I. Ross, A. Savin, W.H. Smith, J. Swanson

University of Wisconsin, Madison, USA

* Corresponding author.
E-mail address: george.alverson@cern.ch (G. Alverson).
† Deceased.
[1] Also at Vienna University of Technology, Vienna, Austria.
[2] Also at CERN, European Organization for Nuclear Research, Geneva, Switzerland.
[3] Also at Institut Pluridisciplinaire Hubert Curien, Université de Strasbourg, Université de Haute Alsace Mulhouse, CNRS/IN2P3, Strasbourg, France.
[4] Also at National Institute of Chemical Physics and Biophysics, Tallinn, Estonia.
[5] Also at Skobeltsyn Institute of Nuclear Physics, Lomonosov Moscow State University, Moscow, Russia.
[6] Also at Universidade Estadual de Campinas, Campinas, Brazil.
[7] Also at California Institute of Technology, Pasadena, USA.
[8] Also at Laboratoire Leprince-Ringuet, Ecole Polytechnique, IN2P3-CNRS, Palaiseau, France.
[9] Also at Suez Canal University, Suez, Egypt.
[10] Also at Zewail City of Science and Technology, Zewail, Egypt.
[11] Also at Cairo University, Cairo, Egypt.
[12] Also at Fayoum University, El-Fayoum, Egypt.
[13] Also at Helwan University, Cairo, Egypt.
[14] Also at British University in Egypt, Cairo, Egypt.
[15] Now at Ain Shams University, Cairo, Egypt.
[16] Also at National Centre for Nuclear Research, Swierk, Poland.
[17] Also at Université de Haute Alsace, Mulhouse, France.
[18] Also at Joint Institute for Nuclear Research, Dubna, Russia.
[19] Also at Brandenburg University of Technology, Cottbus, Germany.
[20] Also at The University of Kansas, Lawrence, USA.
[21] Also at Institute of Nuclear Research ATOMKI, Debrecen, Hungary.
[22] Also at Eötvös Loránd University, Budapest, Hungary.
[23] Also at Tata Institute of Fundamental Research – HECR, Mumbai, India.
[24] Now at King Abdulaziz University, Jeddah, Saudi Arabia.
[25] Also at University of Visva-Bharati, Santiniketan, India.
[26] Also at University of Ruhuna, Matara, Sri Lanka.
[27] Also at Isfahan University of Technology, Isfahan, Iran.
[28] Also at Sharif University of Technology, Tehran, Iran.
[29] Also at Plasma Physics Research Center, Science and Research Branch, Islamic Azad University, Tehran, Iran.
[30] Also at Laboratori Nazionali di Legnaro dell'INFN, Legnaro, Italy.
[31] Also at Università degli Studi di Siena, Siena, Italy.
[32] Also at Purdue University, West Lafayette, USA.
[33] Also at Universidad Michoacana de San Nicolas de Hidalgo, Morelia, Mexico.
[34] Also at Faculty of Physics, University of Belgrade, Belgrade, Serbia.
[35] Also at Facoltà Ingegneria, Università di Roma, Roma, Italy.
[36] Also at Scuola Normale e Sezione dell'INFN, Pisa, Italy.
[37] Also at INFN Sezione di Roma, Roma, Italy.
[38] Also at University of Athens, Athens, Greece.
[39] Also at Rutherford Appleton Laboratory, Didcot, United Kingdom.
[40] Also at Paul Scherrer Institut, Villigen, Switzerland.
[41] Also at Institute for Theoretical and Experimental Physics, Moscow, Russia.
[42] Also at Albert Einstein Center for Fundamental Physics, Bern, Switzerland.
[43] Also at Gaziosmanpasa University, Tokat, Turkey.
[44] Also at Adiyaman University, Adiyaman, Turkey.
[45] Also at Cag University, Mersin, Turkey.
[46] Also at Mersin University, Mersin, Turkey.
[47] Also at Izmir Institute of Technology, Izmir, Turkey.

[48] Also at Ozyegin University, Istanbul, Turkey.
[49] Also at Kafkas University, Kars, Turkey.
[50] Also at Suleyman Demirel University, Isparta, Turkey.
[51] Also at Ege University, Izmir, Turkey.
[52] Also at Mimar Sinan University, Istanbul, Istanbul, Turkey.
[53] Also at Kahramanmaras Sütcü Imam University, Kahramanmaras, Turkey.
[54] Also at School of Physics and Astronomy, University of Southampton, Southampton, United Kingdom.
[55] Also at INFN Sezione di Perugia; Università di Perugia, Perugia, Italy.
[56] Also at Utah Valley University, Orem, USA.
[57] Also at Institute for Nuclear Research, Moscow, Russia.
[58] Also at University of Belgrade, Faculty of Physics and Vinca Institute of Nuclear Sciences, Belgrade, Serbia.
[59] Also at Argonne National Laboratory, Argonne, USA.
[60] Also at Erzincan University, Erzincan, Turkey.
[61] Also at Yildiz Technical University, Istanbul, Turkey.
[62] Also at Kyungpook National University, Daegu, Republic of Korea.